Design and fabrication of tubular reactor for continuous flow synthesis of metal nanoparticles

A project report

Submitted in partial fulfillment

of the requirements for the degree of

Master of Engineering

in the Faculty of Engineering

by

D. Srikanth

Department of Chemical Engineering

Indian Institute of Science

Bangalore 560012 (India)

June 2011

Dedicated

to

My Family

Declaration

I certify that the report was written by myself and the *Departmental Guidelines* were adhered to in preparation of the report/thesis. In writing the report:

1. Experimental data collected by me have been presented without any bias, modifications, or alterations, and can be obtained by others using the information provided in the report.

2. I have not copied material from published/unpublished sources (reports, text books, papers, web sites etc.). I am also aware of the ethical issues involved in writing as per the *Departmental Guidelines*.

3. Where material from any source was used, the source was given due credit by citing it in the text of the report and giving its details in the section on references, and

4. Where material from any source was copied, it was put in quotation marks, and the source was given due credit by citing it in the text of the report and giving its details in the section on references.

(D Srikanth)

Abstract

The physical and chemical properties of metal nanoparticles (1-10 nm) depend on their size and shape. Demand for metal nanoparticles is expected to grow in future because of their wide ranging applications in various fields ranging from medicine to electronics. Commercialization of these applications requires economical synthesis on large scale to meet the future requirements. Recently, various attempts have been made to scale-up the synthesis process using microfluidic reaction technology. Fouling is one of the main disadvantages of microreactors, which hinders the scale-up of synthesis process. In the present work, coaxial flow microreactor has been developed to scale-up and avoid particle deposition. The objective of the present work is to design and optimize the operation of a coaxial flow microreactor to synthesize gold and silver nanoparticles based on the batch protocols developed by Sankar et al. (2009, 2010). This report begins with a brief introduction about nanoparticles and their applications followed by a review of the synthesis of nanoparticles in microreactors. In the next chapter, various attempts made to develop a robust continuous flow process are discussed in detail. This is followed by synthesis of gold and silver nanoparticles in glass and polymer based coaxial flow microreactor. Finally, a summary of the results is presented along with a few recommendations for future work.

Acknowledgement

I would like to thank my Advisor, Dr. S. Venugopal for his able guidance, useful suggestions and encouragement, he had provided during my research work. I want to express my sincere thanks to him for patiently correcting my reports. I am very fortunate to work under him, who taught me so many things which helped me a lot to improve my personal and professional skills.

I would like to thank all the Faculty of Department of Chemical Engineering, IISc for their kindly help in understanding concepts and correcting my misconceptions during my course work. I had the wonderful time and good interaction with them in the class and especially, I cannot forget the joyful environment in the classes of Prof. Kesava Rao and Dr. Sanjeev Kumar.

I would like to thank Prof. Kesava Rao for allowing me to do experiments in his lab and I am also thankful to Prof. S. Subramanian for accessing DLS facility in Department of Materials Engineering, IISc. I am indeed very grateful to Dr. Sanjeev Kumar for changing my attitude towards the problem solving.

I would like to thank all my lab mates Sankar, Girish, Ipshita, Parveen, Vijay, Abhinav and Pearl for their helpful advices and maintaining friendly environment in the lab. I wish to express my sincere thanks to Mohan K Singh for his valuable suggestions to make microchannels.

I am also thankful to Praksh, Mr. Mahadeva Rao, Mr. Venkata, Mr. S. J. H. Samuel (IPC Department) and Mr. Sarvana (CPDM Department) for their valuable assistance during my research work.

I wish to express my sincere thanks to my friends Surya, Sagar, Ganesh, Shiva Mohan Reddy, Shivanand Kumar, Madhav, Sathis, Shital, Tushar, Ravi and all, who made my life in IISc so memorable with a lot of joy.

Lastly, I would like to thank my family for all their love and encouragement throughout my studies, without their constant support this work would not have been possible.

Srikanth Dabbikar

Table of contents

List of figures

List of tables

Chapter 1 Introduction

Nanoparticles are fundamental building blocks for emerging fields like nanomedicine[1], nanoelectronics[2] and nanoarchitecture[3] etc. They are defined as clusters of atoms or molecules in the size range of 1-100 nm[4]. They exhibit different distinctive physical properties like melting point[5], conductivity[6], catalytic activity [7] etc. in comparison with bulk solid, mainly because of their high surface area to volume ratio. Recently, synthesis of metal nanoparticles is gaining importance in nanosciene because of unique optical[8], electrical[2] and catalytic properties[9] of metal nanoparticles . They have applications ranging from cancer treatment[10], bioanalysis[11] to catalysis[12] etc. Self assembly of metal nanoparticles into arrays has applications in data storage[13] and chemo resistive sensors[14] etc. All these applications require synthesis of size controlled metal nanoparticles, due to the size dependent properties.

Synthesis of nanomaterials can be grouped into two approaches namely, top-down and bottom-up[15]. Attrition, milling etc are some of the top-down approaches for synthesis of nanoparticles from large solid chunks, whereas bottom-up approach involves the building of nanoparticles from atoms or molecules in liquid or vapor phase[16]. Bottom-up methods have an edge over top down methods in size control of nanoparticles. Bottom-up methods are typically classified into gas[17] and liquid phase methods[18]. Recently, there is a growing interest in liquid phase methods for synthesis of nanoparticles because it is more energy efficient, rapid, requiring lower capital cost compared to gas phase synthesis methods[16]. In liquid phase method, one of well known strategy for nanoparticle synthesis is the reduction of metal salt into metal atoms to generate supersaturated solutions leading to nucleation , subsequent growth and formation of metal nanoparticles[18](Fig 1.1).These methods are called as traditional beaker methods (Batch mode). Sizes of nanoparticles can be controlled by varying synthesis parameters like concentration, pH of precursors or reducing agent and mode of contacting of reactants[18-20].

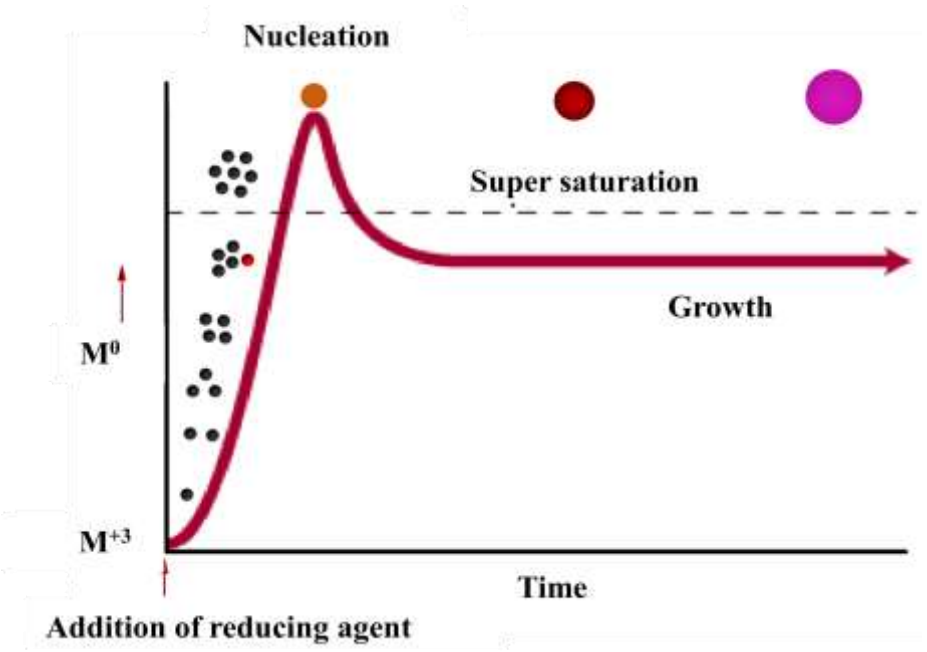

Figure 1.1: Schematic illustrating the variation of metal atom/precursor concentration and nucleation and growth phases of metal nanoparticles. Concentration of metal atoms, which is formed by chemical reaction, increases with time as reaction proceeds. Nucleation occurs when concentration exceeds super saturation. After nucleation, growth of solute results in a decrease in concentration of the metal atoms and growth continues till solute reaches its saturation concentration[21].

However, precise size control is difficult to accomplish because small changes in the above parameters results in unexpected differences in the size distributions. Continuous flow processes can help to overcome the difficulties associated with reproducibility in batch methods[21]. The list of the potential applications of metal nanoparticles expected to grow in the feature, because of their size dependent properties. Commercialization of these applications requires large scale synthesis to meet these future requirements. Continuous flow processes can be scaled-up to produce nanoparticles in bulk quantities[22]. Controlled mixing of precursors can be accomplished through diffusion by reducing dimensions of microreactors[23]. Fouling is one of the main disadvantages of micro reactors, which hinders the scale-up of synthesis process[24]. It can be overcome by either modifying the walls of the rectors[24] or developing new designs[25].

In the present study, we have developed a 3-D coaxial flow microreactor (CFMR) to avoid the particle deposition. The objective of the present work is to develop a robust process using CFMR for continuous flow synthesis of metal nanoparticles.

Chapter 2 Literature survey and Objective

Recently, nanoparticles have been synthesized in microreactors because they have inherent advantages over traditional batch reactors such as precise control on mixing time[21] and rapid heat transfer[22]. As viscous forces dominate over inertial forces in micro reactors, mixing is driven mainly by the processes of diffusion[23]. Microreactors are a promising avenue for scale-up of synthesis process to produce nanoparticles in large quantities and to obtain high quality nanoparticles in reproducible manner[22]. Microreactors are defined as reactors with lateral dimensions in microns (below 1mm). Glass[26], silica[24] and polymers[27] have been used as materials for fabrication of microreactors. Most of the fabrication methods involves soft lithography[27], which is costly and energy inefficient. Molding a polymer around a desired prototypes is a simple, rapid and low cost method for fabricating microchannels[28].

2.1 Capillary based microreactors

Recently, capillary tubes have been used as microreactors[22,29,30] for synthesizing metal nanoparticles (Details are given in Table 1). These types of reactors are easy to fabricate with dimensions of the order of microns. Stainless steel tube[22], Polytetrafluoroethylene (PTFE) tubes[30] and silica glass capillaries[29] have been used as microreactors for nanoparticle synthesis. Due to high heat transfer coefficients, required temperatures to heat the precursor liquids (100-300^{0}C) can be attained within a short period of time (< 1 s) with these reactors[22]. Nanoparticles synthesized in microreactors were found to have an improved polydispersity over batch reactors[30]. The main disadvantage with these types of reactors is the adsorption of nanoparticles on the walls[29]. It has been reported that fouling can be avoided by modifying the surface or by maintaining the solution at certain pH[24].

2.2 Micro fabricated reactors

These reactors are typically fabricated using soft lithography [27]and etching technology[24]. Mixing plays an enormous role in controlling nanoparticles size distribution[21]. It can be improved by modifying the geometry of reactors[31].

Developing a chaotic mixer is one of the approaches for rapid mixing at low Reynolds number[31]. A continuous flow reactor with splitting and recombining units was developed to achieve efficient mixing by changing flow direction of fluid from vertical to horizontal and vice versa[24]. Polydispersity of synthesized nanoparticles improved[24] when compared with batch reactors but these reactors require rapid reducing agents[32] and precise fabrication technology to fabricate microreactors[27].

Table 2.1: Synthesis of nanoparticles in capillary based microreactors

Material used for fabrication	**Type of nanoparticle**	**Poly dispersity**	**Remarks**
Pyrex glass	Gold[29]	17%	Adsorption of nanoparticles on the reactor wall
Stainless steel	Silver[22]	10-20%	High temperature synthesis
PTFE	Silver[30]	10-12%	High temperature synthesis

Table 2.2: Synthesis of nanoparticles in micro fabricated reactors

Type of nanoparticle	**Mixer design**	**Polydispersity**
Gold[24]	Split-recombining	13%
Gold [27]	Radial-interdigiated mixer	20%
Gold[33]	Serpentine mixer	30-35%
Gold[32]	Multi lamination mixer	40%

2.3 Coaxial flow microreactor (CFMR)

A CFMR consists of two concentric cylindrical channels for achieving control on mixing of two miscible fluids through diffusion under laminar regime[25]. Growth and nucleation of nanoparticles can be controlled by reducing the length scales of diffusion or mixing. It is easy to fabricate and operate; diffusion times can be controlled by changing the flow rates of inner and outer fluids and dimensions of outer tube[34]. This geometry helps to avoid problems associated with deposition on the walls[34]. Titanium[34], zeolite A [35], iron oxide [25] and silver nanoparticles have been synthesized in CFMR to avoid clogging and to produce high quality nanoparticles.

Table 2.3: Synthesis of nanoparticles in CFMR

Type of nanoparticle	**Mean size (nm)/Poly dispersity**	**Inner diameter of Inner/outer tube (in mm)**
Titania[34]	100/ 50%	0.6/3
Iron oxide[25]	7/ 16%	0.15/1.7
Zeolite crystals[35]	358/38.7%	0.6/1
Silver[36]	5.1/29%	0.27/2

2.4 Motivation and objective of present work

Synthesis of nanoparticles by reactive crystallization in continuous stirred tank reactor (CSTR) leads to cyclic unsteady state because of back mixing of reactants[37,38]. This means that plug flow reactors are more suitable for scale-up of nanoparticle synthesis. The objective of this project work is to design and optimize the operation of a continuous flow capillary reactor to synthesize gold and silver nanoparticles based on the batch protocols. A room temperature batch protocol was developed for

synthesizing gold and silver nanoparticles using tannic acid as both the reducing agent and stabilizing agent[20,36]. A key finding was that the initial pH of the reactants controlled reactivity, while the final reaction mixture pH controlled the stability of the colloidal dispersion in the case of gold nanoparticle synthesis. Thus, mixing chloroauric acid at a pH of 3.2 with tannic acid at pH of 7.0, rapidly yields gold nanoparticles in the size range of 5 nm[20]. In the case of silver, the pH of silver precursor ($AgNO_3$) does not play a role in the synthesis as long as reaction mixture pH is greater than seven[36].

In present work, coaxial flow microreactor has been proposed to synthesize metal nanoparticles in a reproducible manner under steady state condition. The main advantage of this reactor is that it can avoid particle deposition on the walls. Interfacial reaction between metal salt and reducing agent results in the formation of nanoparticles. Also drop-wise addition of chloroauric acid into a pool of tannic acid resulted in highly monodispersed nanoparticles. So, we decided to mimic this process by having a very thin core diameter such that tannic acid would engulf the gold chloride in the core rapidly, in comparison of reaction time scales. In the present work we focus on low-cost fabrication of CFMR using polymer and glass as the materials of construction and on studying the effect of various solution parameters like molar ratio, pH and concentration and, flow parameters such as flow rate and flow rate ratio on the particle size distribution of metal nanoparticles produced in continuous manner.

Chapter 3 Results and Discussion

First, this chapter discusses the various stages of the design process for fabricating a CFMR using Perfluoro alkoxy alkane (PFA) capillary tubes and the results of various trouble–shooting exercises undertaken to overcome some of the challenges. It then presents the results of experiments carried out to synthesize gold nanoparticles in a continuous manner, and finally concludes with discussion on the plausible reasons for the observed size distribution.

3.1 Fabrication of CFMR and trouble-shooting

Polymer and glass capillary tubes were used as material for fabricating CFMR and the reactor set up consists of two concentric tubes; namely inner tube (50 µm ID, 360 µm OD, PFA tube) and outer tube (2.4 mm ID, 4 mm OD, glass tube). Micropipette tips were used for precise centering of PFA tube in outer tube (Fig 3.1). Inlet port for the outer fluid was designed such that it was perpendicular to the main flow direction (Fig 3.1). COMSOL multi physics software was used to perform numerical simulations of Navier-Stokes equation to determine ratio of volumetric flow rates between inner and outer flows required in order to maintain fully developed coaxial laminar flow[26]. Simulation results showed that outer fluid flow rates should always be greater than ten times of inner fluid flow rates to maintain inner fluid core diameter as thin as possible[26].

Initially, Flow visualization experiments were conducted with dye and water maintaining a flow rate ratio of 1:12 (Inner: Outer) at a total volumetric flow rate of 39 mL/h in CFMR. Homemade syringe pumps were used for pumping liquids through inlets of the reactor. Initially, the flow was observed to be coaxial in nature. After some time, a shifting of dye stream from the point of confluence and oscillations at the point of confluence were recorded (Fig 3.2). The plausible reason for this behavior may be instabilities related to the tangential velocity component of the fluid fed in the inlet for outer fluid flow. To avoid this, the Inlet of outer fluid was modified by providing a bulb (25 mm diameter) between inlet of outer fluid and outer glass tube (Fig 3.3).

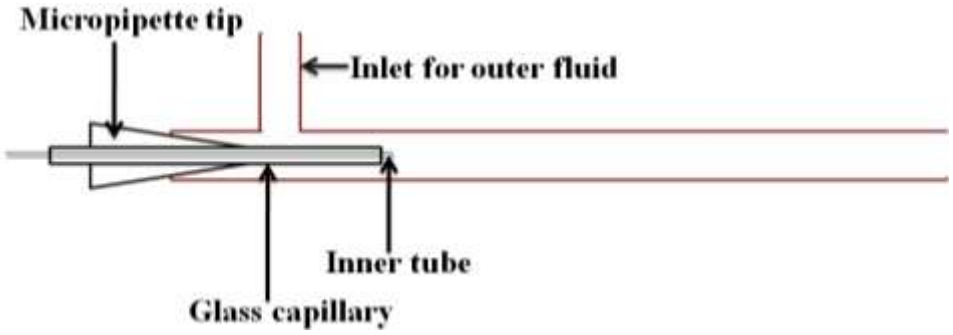

Figure 3.1: Schematic showing CFMR-I fabricated using a PFA capillary as an inner tube and glass tube as the outer tube. Set up consists of three fluidic ports; two of them were inlets for inner and outer fluid, while another one was for the outlet.

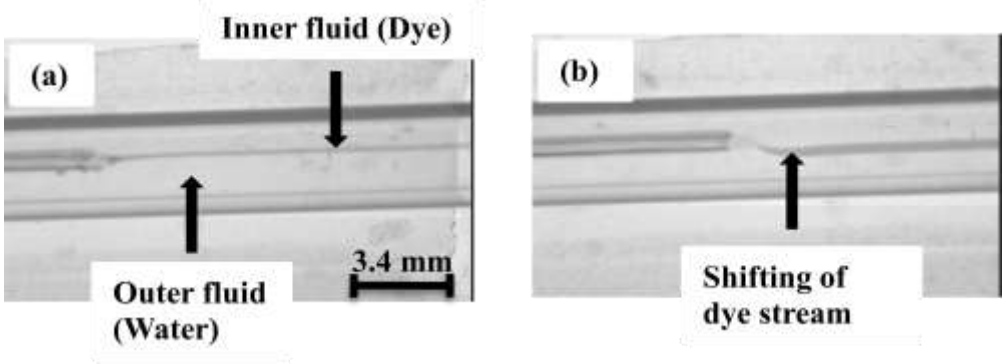

Figure 3.2: Digital micrographs of flow visualization experiments conducted in CFMR-I (a) at t=0 (b) t=5 min. Displacement of dye stream from point of confluence was observed after a certain time possibly, due to instabilities associated with outer tube fluid.

Flow visualization experiments carried out in CFMR-II again at same operating conditions mentioned earlier. Surprisingly, same kind of flow behavior (oscillations) was observed and even a change in operating conditions (0.6 mL/h for inner fluid and 36 mL/h for outer fluid) did not result in a change of the observed phenomena. We surmised that oscillations of syringe pumps may be responsible for this observed behavior. Gravity flow to CFMR rather than syringe pumps was employed to pump the liquids in further experiments. The inner diameter of inner tube was increased from 50 µm to 400 µm in order to track the disturbances easily. Oscillations were

again observed at the point confluence. This observation clearly confirmed that, this behavior is due to external vibrations and not because of syringe pumps. Finally, the source of the disturbances was identified to be the acoustic noises generated by the air handling unit of the clean room in Lab 2A. To avoid this noise, all further experiments were carried out in a relatively quiet corner of Lab 2 and visualization experiments (Fig 3.4) confirmed the steady nature of flow.

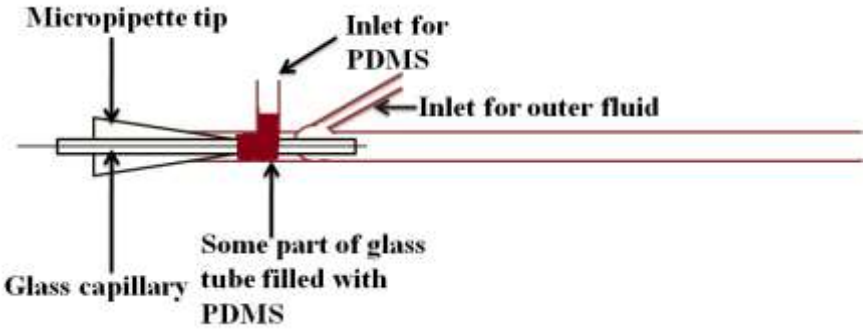

Figure 3.3: Schematic diagram of CFMR-II. Conical shape of micropipette tip allows for the precise centering of inner tube in outer tube. Additionally, embedding the micro pipette tip in PDMS enhanced its mechanical strength. The Inlet of outer fluid was modified by providing a bulb (25 mm diameter) between inlet of outer fluid and outer glass tube in order to enable proper converging flow through outer tube.

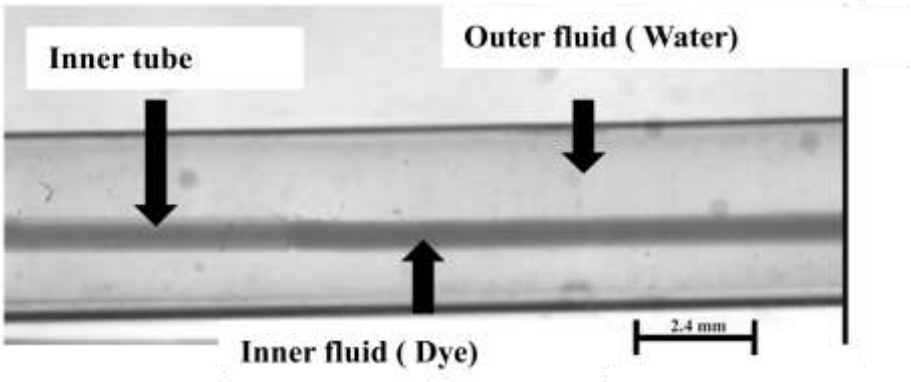

Figure 3.4: Snapshot of dye flowing in CFMR-II. Dye stream flowed steadily through the inner tube without any oscillations. Inner diameter of inner tube is around 400 μm, flow rates were used 3 mL/h for inner fluid and 36 mL/h for outer fluid.

Another important aspect of the fabrication process was the need for precise centering of the inner tube. Fig 3.5 and 3.6 shows that the inner flow behaves like a jet and hit the bottom of the capillary tube, if it is not properly centered. To avoid this issue, a polydimethyalsiloxane (PDMS) based inlet manifold (Fig 3.7, See appendix A.2 for details) was designed to allow precise centering of the inner tube and provide sufficient mechanical strength.

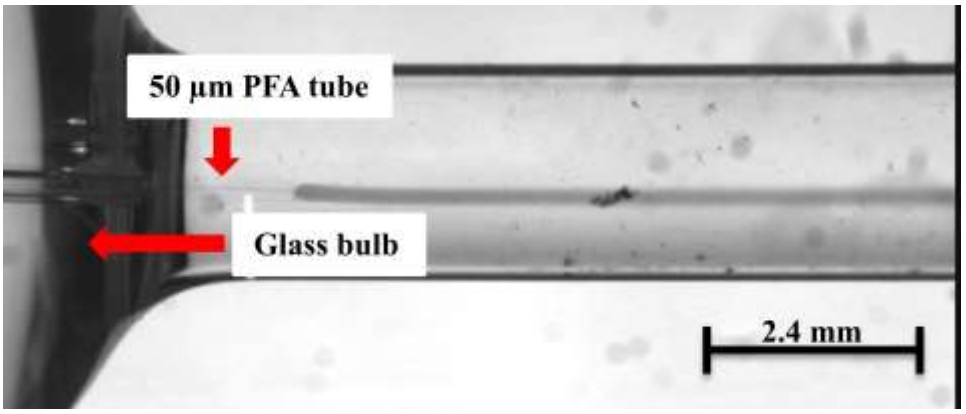

Figure 3.5: Snapshot of CFMR-Design 2 at the entrance. Co axial flow was maintaining up to certain length in CFMR.

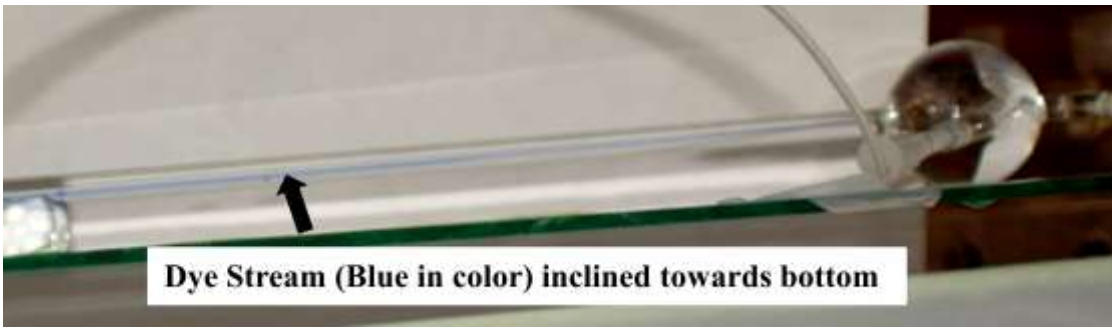

Figure 3.6: Flow visualization experiments in CFMR-Design 2. Coaxial flow maintained up to certain distance only. Dye is expected to flow in center but it flows like a jet to the bottom (due to inaccurate centering of inner tube).

Figure 3.8 shows that the flow is now coaxial as expected. The width of inner flow (dye appears as black) was measured using the grey scale profile (Fig 3.8 inset) along the line shown in Fig 3.8 and compared to the value expected based on coaxial laminar flow, neglecting diffusion (see appendix A. 3 for details). The measured width was 300 µm, while the calculated value was 200 µm. This discrepancy is attributed to inevitable errors associated with the imaging and image analysis processes. We note that the inner core diameter is the relevant diffusion length scale in our reactor.

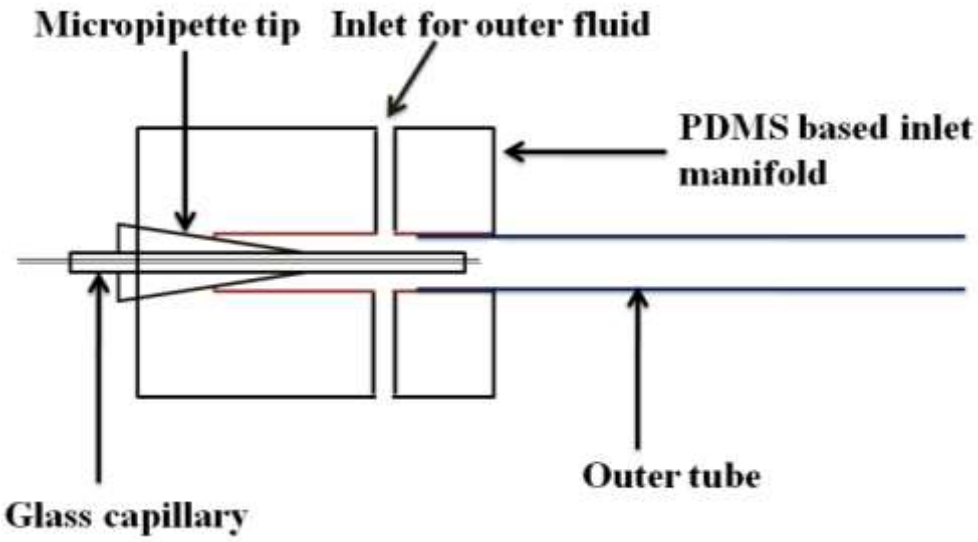

Figure 3.7: Schematic diagram PDMS module-CFMR.

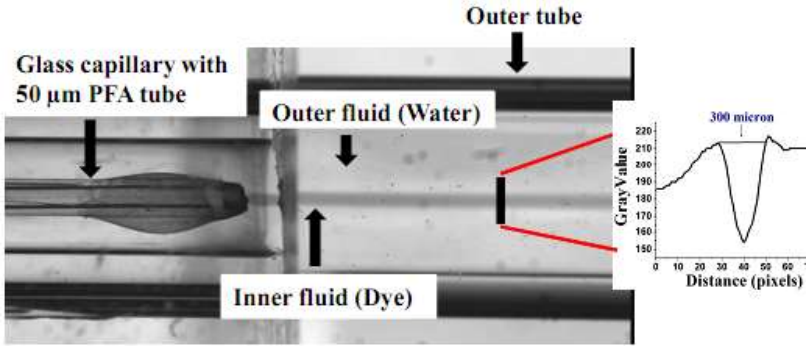

Figure 3.8: Snapshot of flow visualization experiment in coaxial flow microreactor. The inset shows the grayscale profile (1 µm = 0.06 pixels) along the black line shown in Fig 4.8.

3.2 Gold nanoparticle synthesis

Synthesis of gold nanoparticles was carried out in CFMR-III (PDMS inlet manifold) by using tannic acid protocol at room temperature[20]. Aqueous chloroauric acid (0.6 mL/h) at a concentration of 0.25 mM was fed through inner tube , while reducing agent (tannic acid) at a concentration of 0.09 mM was fed (36 mL/h) through outer tube in this reactor. Initially, tannic acid fills the entire tube, while gold chloride is separated from the contents of the outer tube by a small plug of water, pumped just prior to injection of chloroauric acid. The reaction between two reactants results in formation of gold nanoparticles. Overall molar ratio of tannic acid to gold salt (based on final collected volume) was maintained at 2.08 in CFMR, similar to the batch process to compare the results. Gold nanoparticles were collected in petri dish at different time intervals to examine the dynamics of the reactor. Visible spectra (Fig 3.9) showed the presence of gold nanoparticles exhibiting surface plasmon resonance at 528 nm.

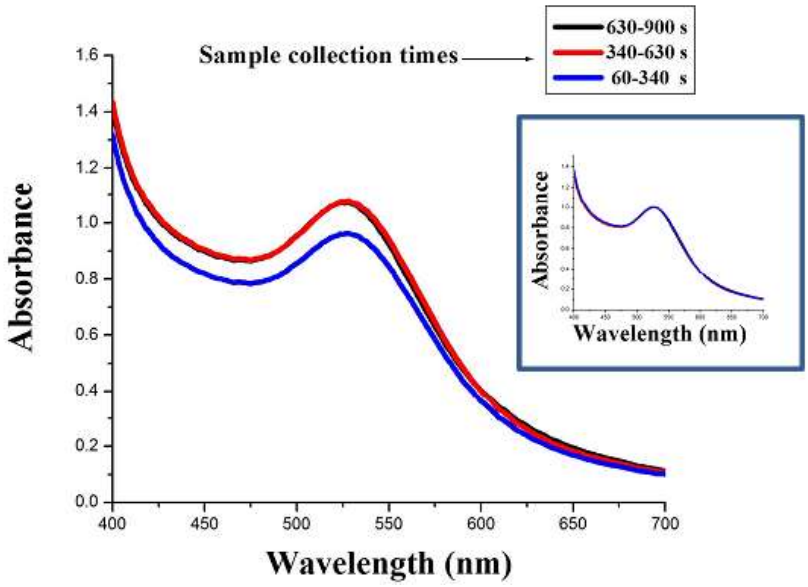

Figure 3.9: Visible spectra of gold nanoparticles synthesized in CFMR. Gold nanoparticles samples were collected to check the dynamics of the reactor. Coincidence of normalized visible (as shown in inset) spectra of gold nanoparticle samples confirms the steady state nature of the process.

Visible spectrum of gold colloid is identical for samples collected between 630-900 s and 340-630 s. Visible spectrum of gold colloid sample collected between 60-340 s has lower absorbance than the other samples; the reason for this behavior is possible dilution of gold nanoparticles with excess tannic acid during the startup phase. The normalized plots shown in the inset confirms the steady state nature of the process. We note that this is the first report of steady state continuous flow synthesis of gold nanoparticles. Tannic acid charge stabilized gold nanoparticles are difficult to image with FESEM (Field emission scanning electron microscopy) because of organic contamination. It is necessary to stabilize gold nanoparticles with alkane thiol and to transfer to organic phase. 5 mL of the product gold nanoparticles, 5 mL of ethanol and 1 µL of dodecanethiol were mixed in a centrifugal tube and centrifuged for 30 min to obtain a precipitate after two hours. Ethanol was used to wash this precipitate to remove excess surfactants and then it was allowed to dry overnight in the laminar hood. The dried thiol-capped gold nanoparticles were redispersed in 0.5 mL chloroform. 2 µL of this concentrated gold nanoparticle sample was placed on a cleaned silicon wafer piece for analysis under FESEM.

A further experiment was carried out at a chloroauric acid concentration of 0.05 mM (MR-10.4) to understand the role of concentration of precursors. Figure 3.11 shows that steady state is achieved for these conditions also. To compare these results with batch reactors, two controlled experiments were carried out in batch reactors with and without mechanical agitation. We expect the batch process (without agitation) in which a jet of chloroauric acid is injected into a stationary pool of tannic acid to mimic the mixing present in the continuous flow reactor. Overall molar ratio and volume of reactants were maintained same as CFMR for direct comparison. Distinctive difference in UV-Vis spectra for different contact modes confirms that variation in mean size (Fig 3.10). Size distribution of nanoparticles synthesized in CFMR, batch-with agitation and batch-without agitation were found to be 10.2 ± 4 nm, 10.4 ± 3.8 nm and 6.5 ± 1.5 nm (Fig 3.12) at MR 2.08 and 5 ± 1.5 nm, 5.8 ± 1.9 nm and 4.8 ± 1.7 nm (Fig 3.13) at MR 10.4. These results are summarized in Table 4.1.

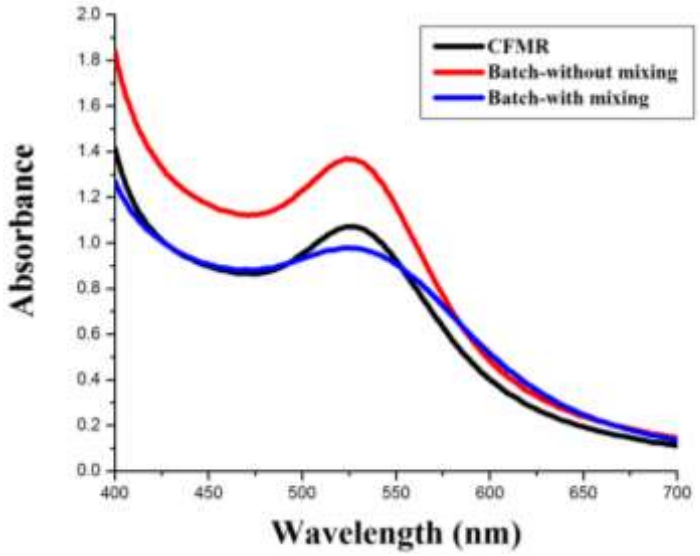

Figure 3.10: Visible spectra of gold nanoparticles synthesized through different contact modes namely CFMR, batch without agitation and batch with agitation for comparison at MR 2.08. Difference in visible spectrum is clearly indicates that difference in gold nanoparticles size distribution.

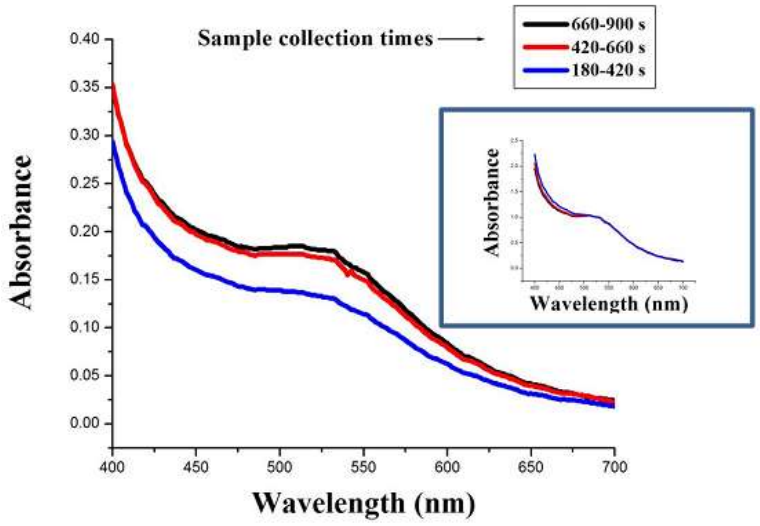

Figure 3.11: Visible spectra of gold nanoparticles synthesized in CFMR (MR 10.47).Gold nanoparticles samples was collected at different time intervals to verify the dynamics of the process. Coincidence of normalized plots confirms the steady state nature of the process (inset).

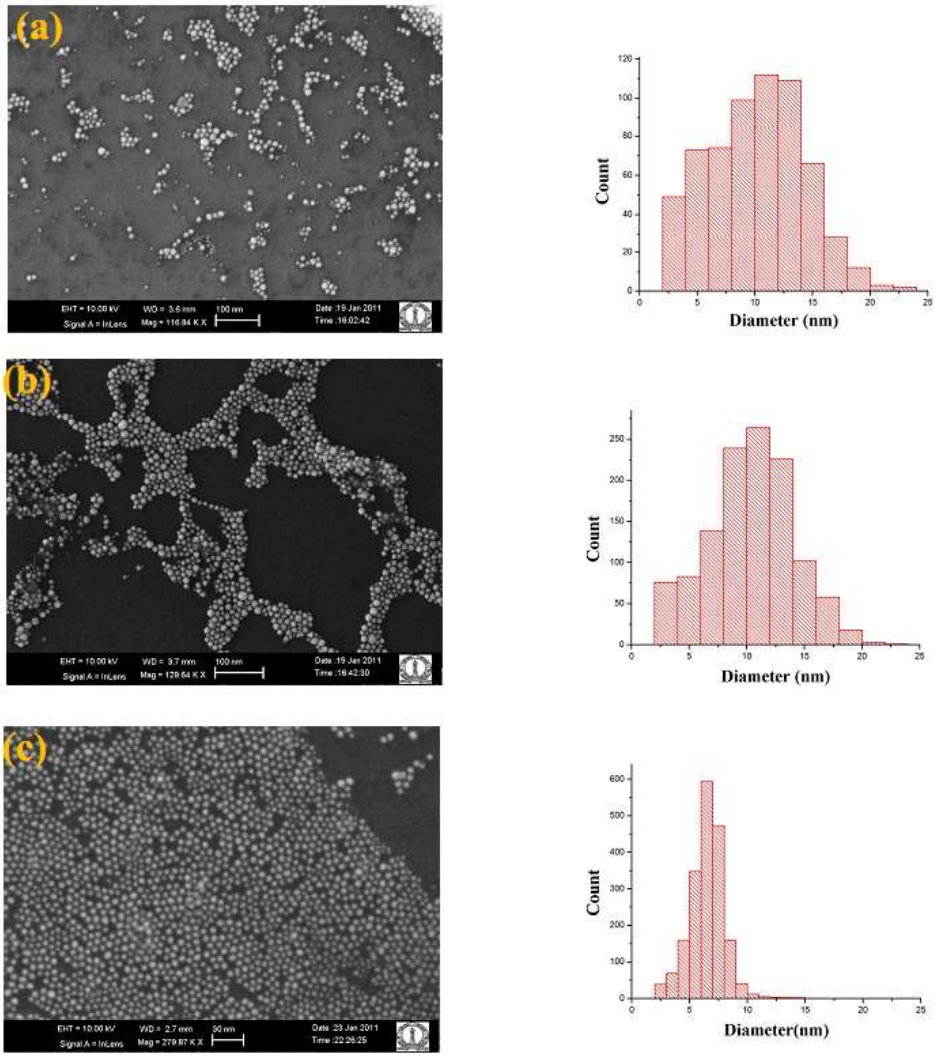

Figure 3.12: Representative FESEM images of gold nanoparticles synthesized through different contact modes (Left) and size distribution histogram of nanoparticles obtained using Clemex@ software (right).(a) CFMR, Nanoparticle diameter 10.2 ± 4.2 nm. (b) batch-without agitation, Nanoparticle diameter 10.4 ± 3.8 nm. (c) batch-with agitation, Nanoparticle diameter 6.5 ± 1.5 nm. pH of chloroauric acid was 1.4 and pH of tannic acid solution used was 7.1 in all these experiments.

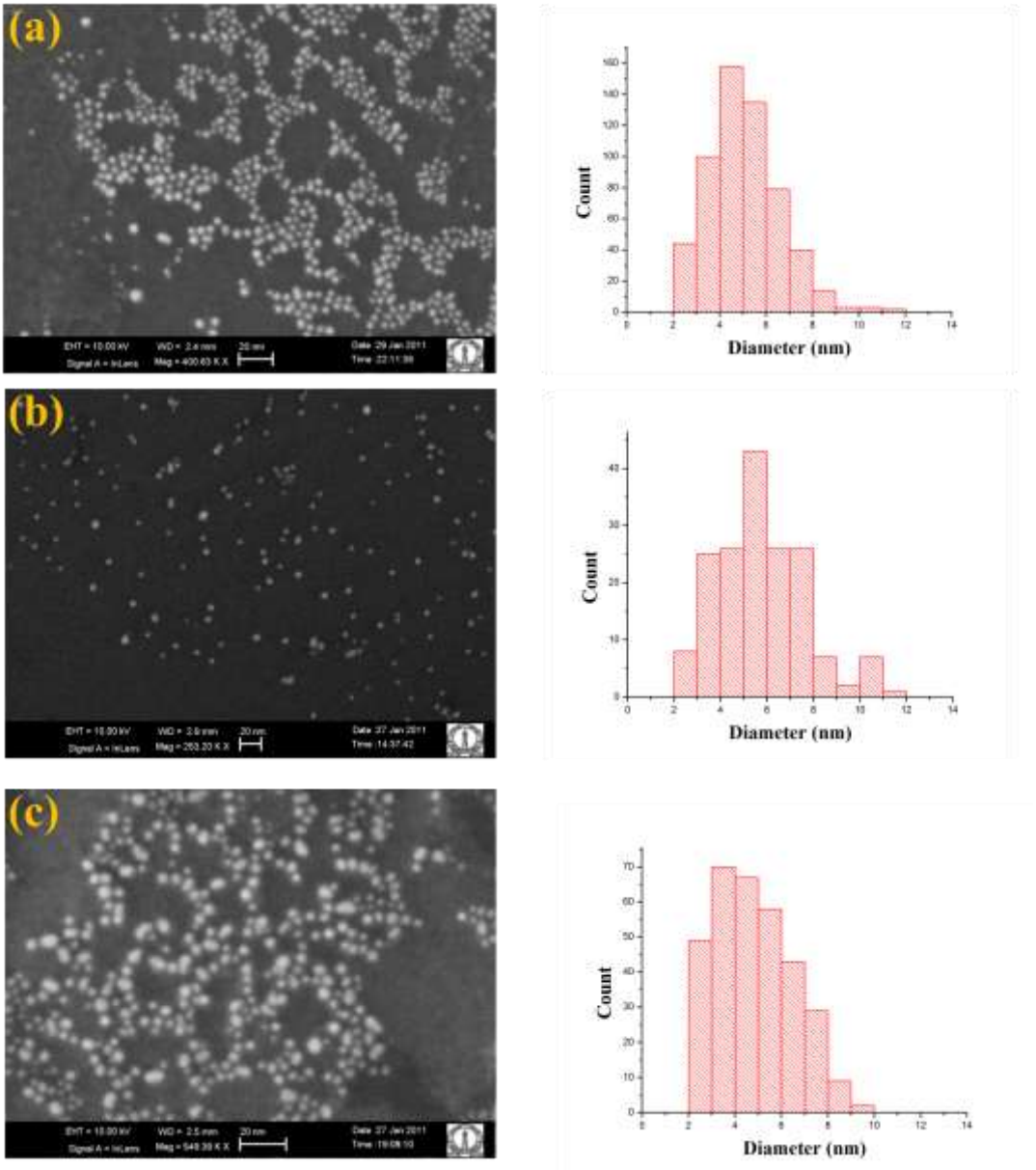

Figure 3.13: Representative FESEM images of gold nanoparticles synthesized through different contact modes at molar ratio (tannic acid/chloroauric acid) 10.4 (Left) and corresponding size distribution histogram of nanoparticles obtained using Clemex@software (right). (a) CFMR, Nanoparticle diameter 5 ± 1.5 nm. (b) batch-without agitation, Nanoparticle diameter 5.8 ± 1.9 nm. (c) batch-with agitation, Nanoparticle diameter 4.8 ± 1.7 nm. pH of chloroauric acid at 2.5 and pH of tannic acid at 7.1 maintained in all these experiments.

3.3 Discussion

Gold nanoparticles were synthesized at two different molar ratios. Triangular nanoparticles and wide size distribution was observed when chloroauric acid concentration 0.25 mM. The plausible reason for this behavior is that nanoclusters, which are produced near the contact region, can diffuse either in basic medium or acidic medium. Decomposition of unreacted chloroauric acid results into formation of chloride (Cl^-) ions and they can etch the surface of gold nanoclusters, which are growing in acidic medium leading to formation of triangular nanoparticles[39] (Fig 3.14). The spherical shape of nanoparticles observed when gold concentration was 0.05 mM to support this hypothesis.

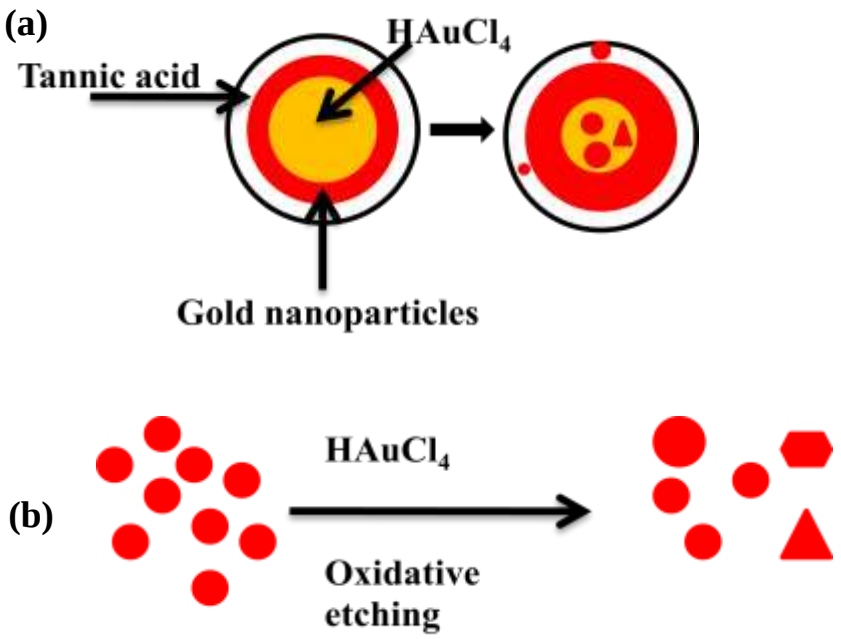

Figure 3.14: Schematic illustrating the reason for triangular nanoparticles when chloro auric acid concentration 0.25 mM (MR-2.08). (a) Nanoclusters, which are formed during initial stage, can diffuse either into acidic or basic medium and nanoparticles which are in basic medium are better stabilize by tannic acid. (b) Oxidative etching gold nanoclusters by chloride ions leads into formation of triangular nanoparticles.

The particle size distribution results (table 3.1) indicate that bulk mixing plays an important role at higher chloroauric acid concentrations (and low MR values) and that mean size and distribution can be controlled by changing the precursor concentrations. From a production stand point, the processing rates were in the range of 1-10 mg/h of gold, which is comparable to those reported in the literature[24,29]. During the preliminary experiments, the overall flow rates were constrained due to the flexible nature of PFA (inner tube). So, a further modification was made in the fabrication process, wherein silica capillary tube was used for inner tube in conjunction with a PDMS input manifold and tube for the outer flow. These experiments are discussed in the next chapter.

Table 3.1: Size distribution of gold NPs synthesized in CFMR at two different molar ratios.

Molar ratio	**Contact mode**	**Size distribution (nm)**	**Coefficient of variance (COV)**	**Remarks**
2.08	CFMR	10.2 ± 4.2	41%	Triangular nanoparticles (few)
	Batch-with agitation	6.5 ± 1..5	23%	
	Batch-without agitation	10.4 ± 3.8	37%	Triangular nanoparticles (few)
10.4	CFMR	5.0 ± 1.5	33%	
	Batch–with mixing	4.8 ± 1.7	35%	
	Batch-without mixing	5.8 ± 1.9	30%	

Chapter 4 PDMS based coaxial flow micro reactor

Polydimethyalsiloxane (PDMS) is soft and flexible polymer widely used for fabricating microchannels[28]. Fabrication of microchannels with PDMS has received wide attention due to their optical properties[40], ease of bonding[41], good thermal [28]and oxidative stability[42] etc. Soft lithography based on the PDMS is one of the emerging cost effective technologies for micro fabrication. A rapid PDMS microchannel fabrication method was developed by molding PDMS around nylon threads[28]. In present work, this particular method has been used for fabrication.

4.1 Fabrication of microchannel

Different diameters of microchannels were fabricated by glass rods with different diameters and needles with various sizes as a channel molds (Fig 4.1). Glass rods (needles) were kept between the two rigid supports in microchannel mold. Bubble free PDMS, which is the mixture of SYLGARD 184 silicone elastomer base and curing agent (10:1 by weight), was poured in the microchannel mould. It was then kept in an oven for curing at $60^{o}C$ for four hours. After curing, Hexane and heptane were used to swell the PDMS cross linked network to remove the glass rod or needle from it. PDMS block was allowed to deswell in ethanol and followed by five hours of continuous heating in oven at $60^{0}C$ to evaporate ethanol and heptane solvents from it.

Coaxial flow microreactor consists of two concentric tubes namely inner and outer tube (Fig 4.2) and the mixing of two miscible fluids performed through diffusion. Outer tube with 1.1 mm ID was fabricated by molding PDMS around 1.1 mm glass rod. Inner tube with 150 µm ID and 360 µm OD is made out of fused silica was inserted in the center using two concentric micro pipette tips, which are attached to the outer capillary. Flow visualization experiments (Fig 4.3) were carried out to visualize flow patterns in CFMR with dye as inner fluid and water as outer fluid. Volumetric flow rates of outer and inner tube maintained at 60:1, 30:1, 12:1 ratios in these experiments.

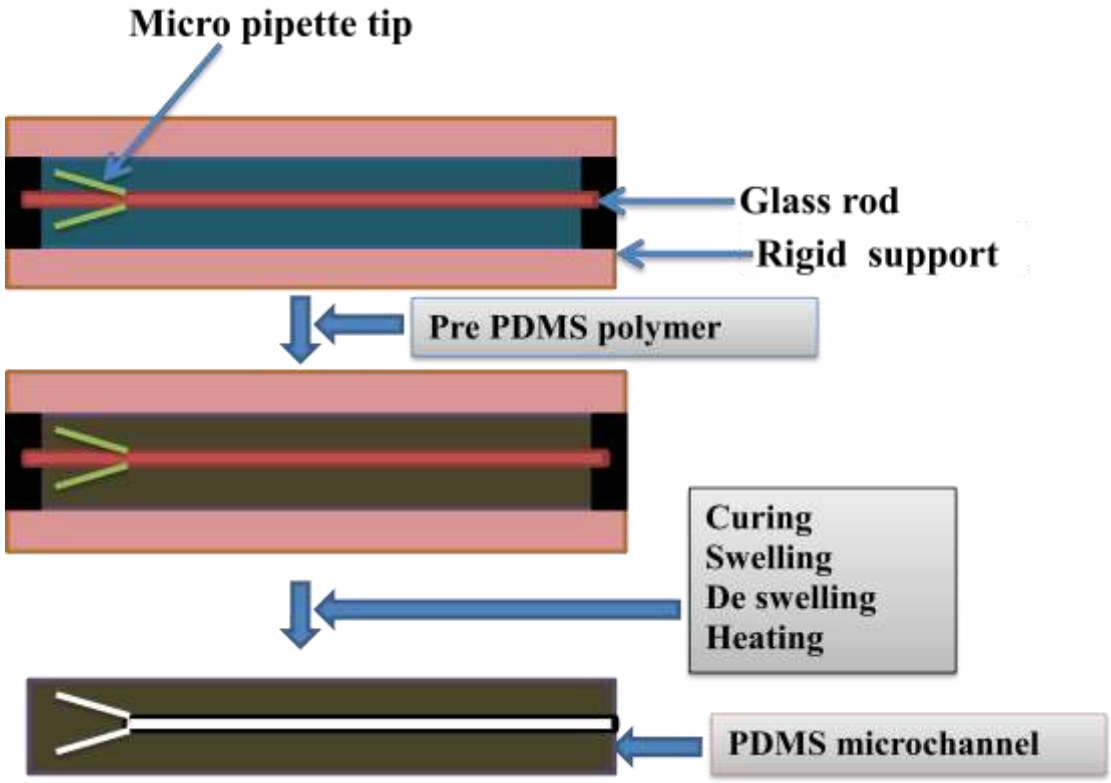

Figure 4.1: Schematic illustrating the procedure for fabrication of microchannel through PDMS as a material. Glass plate (3 cm width and 20 cm length) was used as a rigid support and two glass plates with 1cm width, 1.5 cm thickness and 20 cm length kept apart with distance of 1 cm on the top of it to create space to hold desired molded shape. Pre polymer liquid was poured around a glass rod; curing, swelling, de swelling and heating is the next steps to fabricate microchannel with 1mm diameter.

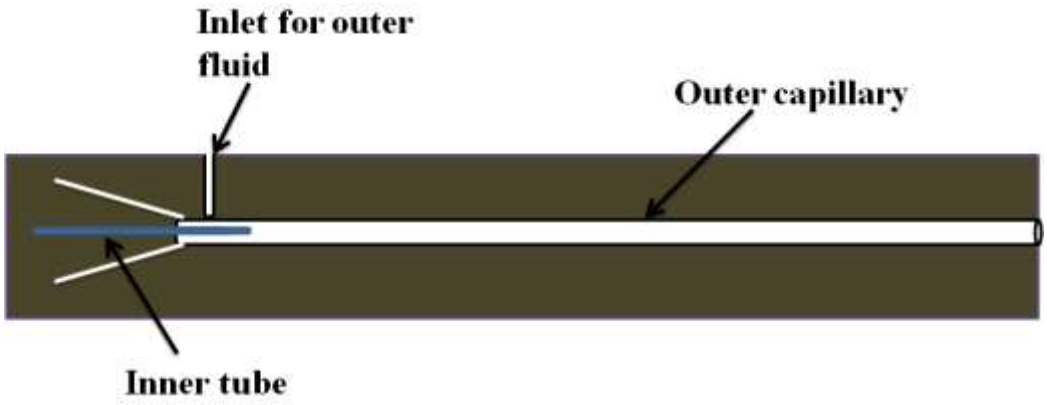

Figure 4.2: Schematic showing the PDMS based coaxial flow microreactor.

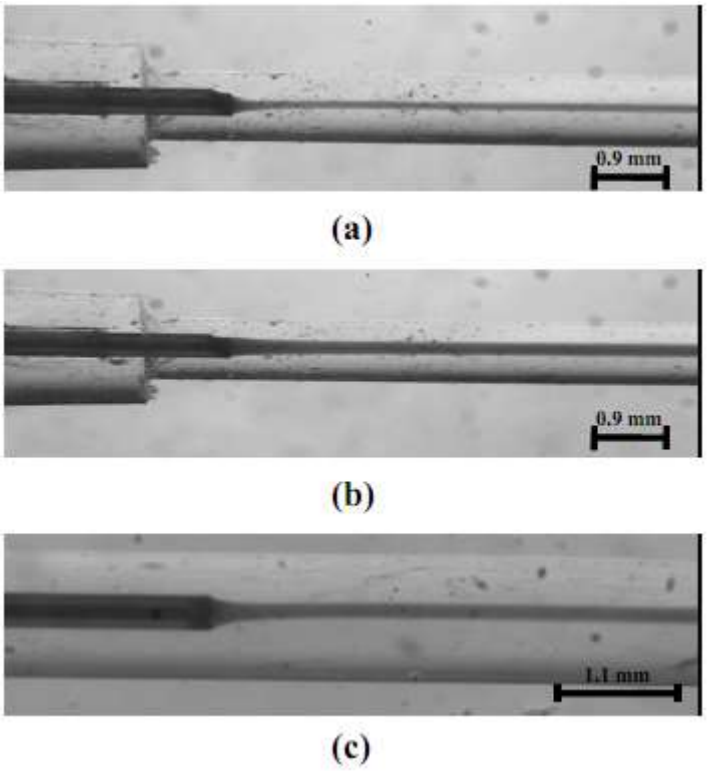

Figure 4.3: Snapshots of flow visualization experiments conducted in 0.9 mm and 1.1 mm CFMR. Experiments were carried out at different volumetric flow ratios. Experimental core diameter of inner fluid calculated from by Image J software. (a) 0.9 mm microchannel at 60:1(O/I) flow rate ratio, Inner core diameter 100 µm. (b) 0.9 mm microchannel at 30:1 flow rate, Inner core diameter 150 µm. (c) 1.1 mm microchannel at 60:1 flow rate,120 µm .

4.2 Synthesis of silver nanoparticles

Silver nanoparticles were synthesized in CFMR (1mm ID outer tube, 0.15 mm ID inner tube and 135 mm length) at overall molar ratio of tannic acid to silver nitrate of 0.068 at different flow rates. Volumetric flow rates of two reactants were maintained at 60:1 (Outer: Inner) in order to reduce the core diameter (0.12 mm) of inner fluid in coaxial flow to decrease the diffusion timescales of both the reactants. Silver nitrate (0.423 mM) fed through inner tube whereas tannic acid (0.093mM,pH 8) through outer tube at different overall flow rates ranging from 30.5 mL/h to 91.5 mL/h. Reaction between silver nitrate and tannic acid results in formation of silver nanoparticles. Yellow color appearance of silver nanoparticles (grey line) was observed in CFMR (Fig 4.4). The appearance of color starts at a length (measured

from point of confluence), which corresponds to a residence time of 1 s. This time correlates well with time scales of reaction measured in batch reactors[36].

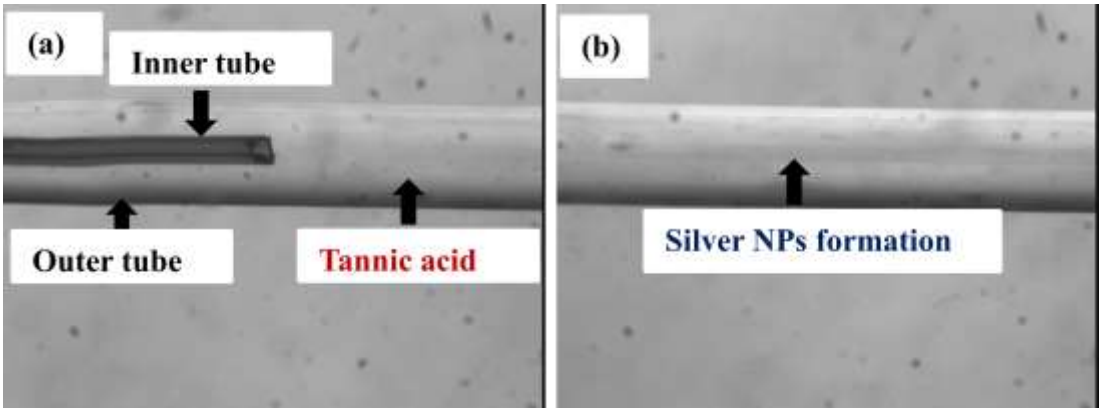

Figure 4.4: (a) Snapshot of co axial flow micro reactor, which is used for synthesizing silver nanoparticles. (b) Silver nanoparticles (grey line) are formed due to interfacial reaction between tannic acid and silver nitrate. Appearance of yellow color within the reactor starts after 3 cm distance from the point of confluence, corresponds to the residence time of 1 s (91.5 mL/h flow rate).

The samples were collected in petridish at different times to verify the dynamics of the reactor as well as for further characterization techniques (Fig 4.5). UV-Visible spectra of silver nanoparticles showed the presence of silver nanoparticles by exhibiting the surface plasmon resonance in the visible region at 410 nm (Fig 4.6). Two more peaks were observed along with silver corresponded to the tannic acid at 205 nm and 260 nm. Coincidence of normalized plots (UV-Vis spectra) confirmed the steady state nature of the process (Fig 4.6 inset). Experiments were repeated for reproducibility of the results. Samples were analyzed with UV- Spectrophotometer. It showed that UV-Vis spectrum was similar for both trials (Fig 4.7). There is no significant difference in the UV-Visible spectra of silver nanoparticles synthesized in CFMR at different flowrates (Fig 4.8).

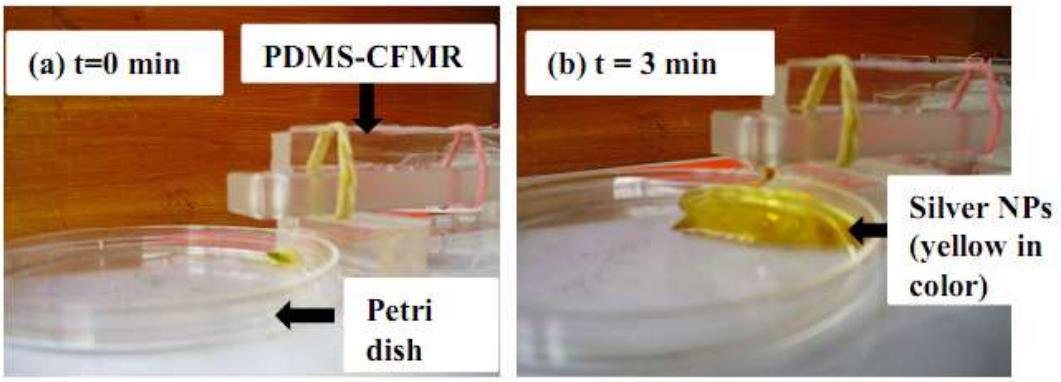

Figure 4.5: Snapshots of silver nanoparticles synthesized in CFMR. Samples of silver nanoparticlescollectedg in petridish at different times to verify the steady state of continuous flow proces.

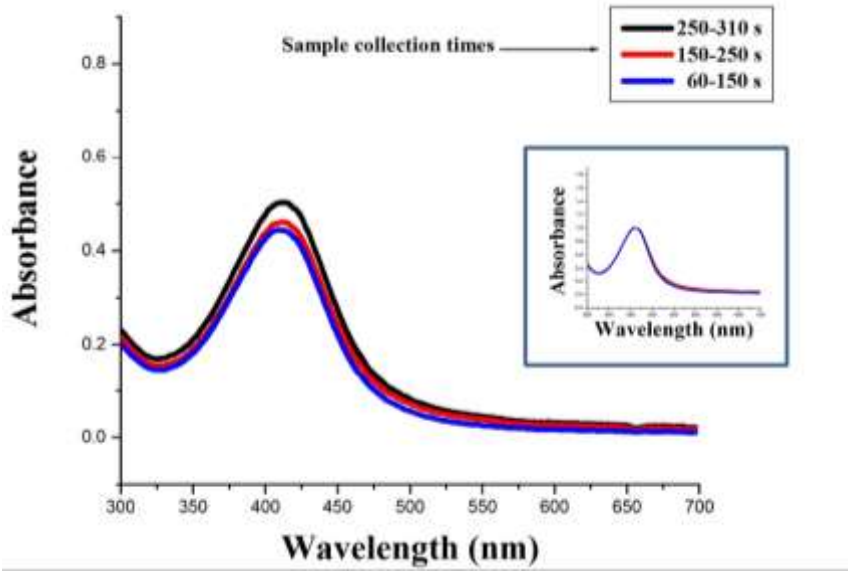

Figure 4.6: UV-Visible spectra of silver nanoparticles synthesized in PDMS based CFMR (inner tube 150 micron). Silver nanoparticles samples were collected to check the dynamics of the reactor. The inset shows normalized plots. The overlapping of normalized UV-Vis spectra of samples collected at various time intervals verifies the steady state nature of the process.

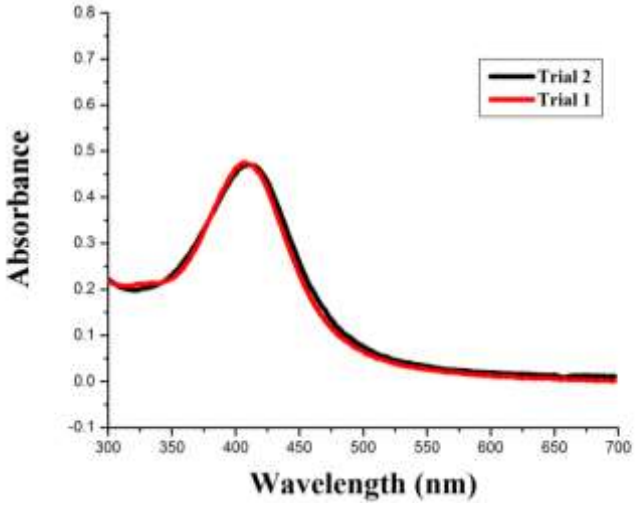

Figure 4.7: UV-Visible spectra of silver nanoparticles synthesized in CFMR by maintaing tannic acid at 54ml/hr flow rate where as silver nitrate at 0.9 ml/hr and similar concentrations employed in both the cases. Both the experiments were conducted to verify the reproducibility of experiments. Coincedence of UV–Visible spectrum of both trials indicates that experimets are reproduciable.

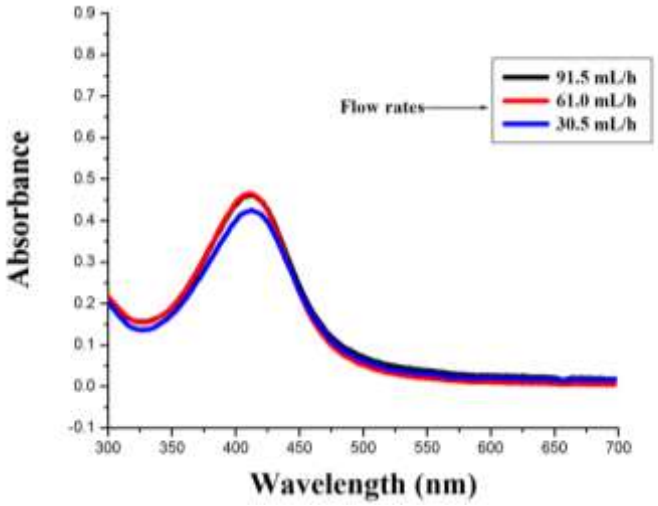

Figure 4.8: UV-Vis spectra of silver nanoparticles synthesized in CFMR at different flow rates. Surface Plasmon resonance of silver showed at 410 nm. These spectra show that particle mean size remains same because there is no significant difference in spectra.

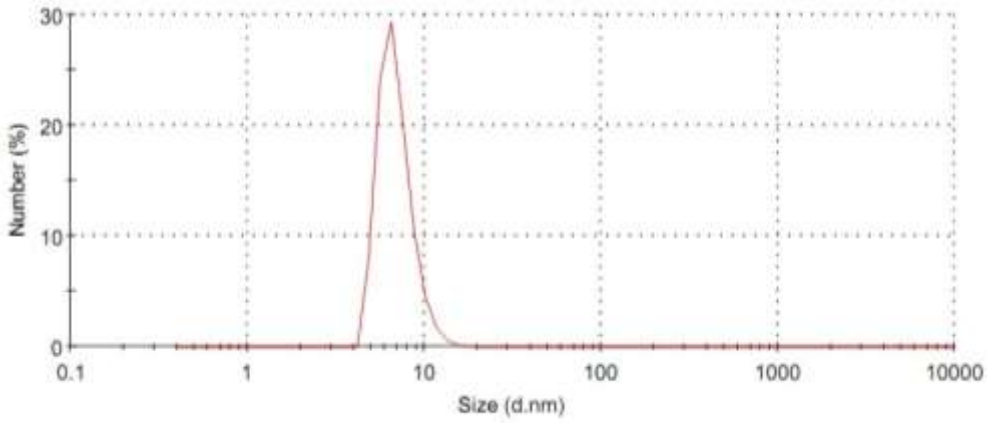

Figure 4.9: Size distribution of silver nanoparticles synthesized in CFMR (90 mL/h flow rate - tannic acid and 1.5 mL/h flow rate - silver nitrate) obtained by Zetasizer in terms of number (%). It found to be 6.9 ± 1.6 nm.

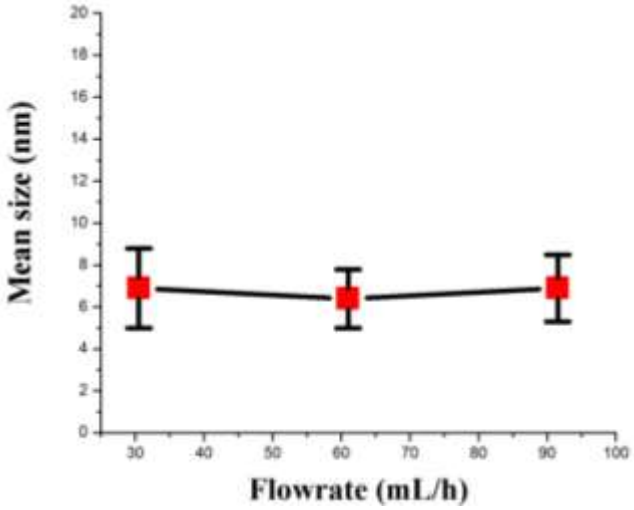

Figure 4.10: Variation of hydrodynamic diameter of silver nanoparticles synthesized in CFMR with different flow times. The error bars represents standard deviation.

Size distribution of silver nanoparticles samples obtained by DLS (Dynamic Light Scattering) is show in Fig 4.9. These results show that particle size distribution is independent of flow rate (Fig 4.10). This is advantageous for scheduling different

production rates and in simplifying the control equipment required, as the quality of colloidal solution is mainly related to the nanoparticle size distribution.

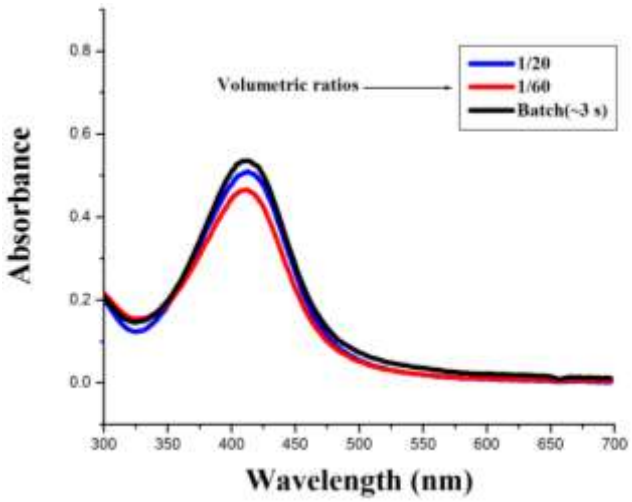

Figure 4.11: UV-Visible specta of silver nanoparticles synthesized in CFMR at different volumetric ratios.

Mixing is completely driven by diffusion in coaxial flow microreactor and diffusion time scales can be controlled through varying the flow ratios in CFMR. Inner fluid core diameter was increased to 180 µm from 120 µm by varying the volumetric flow ratio from 1:60 to 1:20 in order to increase the diffusion time (3.6 s-9 s). Silver nanoparticles were synthesized by maintained at molar ratio of tannic acid to silver nitrate at 0.068 for easy comparison with batch. UV-Visible spectrum confirms that there is no significant difference in particle size (Fig 4.11) and particle characterization with DLS was also shows that mean size of nanoparticle remain constant (summarized in Table.4.1). The size of particles synthesized was similar to the batch process indicating that diffusion time scales are not critical.

Table 4.1: Particle size distribution at different mixing times

Contact mode	**Mixing time (s)**	**Particle size distribution (nm)**
Batch	3 s	5.6 ± 1.8
CFMR (1/20)	9 s	7.7 ± 2.2
CFMR (1/60)	3.6 s	6.4 ± 1.4

4.3 Synthesis of gold nanoparticles

Gold nanoparticles were synthesized in coaxial flow microreactor (1mm ID outer tube, 0.15mm ID inner tube and 135 mm length) using chloroauric acid as a precursor and tannic acid as reducing and stabilizing agent. Molar ratio of tannic acid to chloroauric acid was maintained at 2.08 for easy comparison with batch. Chloroauric acid (0.25 mM) was fed through inner tube with 0.75 mL/h and where as tannic acid (0.05 mM pH 7) was fed through the outer tube with 45 mL/h. Chloroauric acid pH was maintained between 1.8-2.4 and tannic acid pH at 7 in order to maintain overall reaction mixture pH above 6 to minimize coalescence. UV-Visible spectrometer and scanning electron microscopy were used for particle characterization. Gold nanoparticle samples were collected at different time levels to verify the dynamics of the reactor (Fig 4.12). Coincident of UV-Vis spectra of samples collected at various time intervals (300-500 s, 500-700 s) verifies the steady state nature of the process.

The size distribution of gold nanoparticles were found to be 10 ± 3.9 nm,8.2 ± 3.4 nm, 6.5 ± 3.0 nm when overall concentrations of gold salt were 0.05 mM.0.25 mM,0.5 mM respectively(Fig 4.14). Mass balnce of gold nanoparticles based on mean diameter,which is obtained from SEM images (Fig 4.14),indicates that the number of nanoparticles are more in the case of higher concentrations compared to lower concentrations.It is also well known that initial nucleation rate is high for higher concentrations and rate of coalscence of intial nuclei is more in the case of higher concentration compared to lower concentration.These facts suggest that coalscence play key role in determining the particle size (Fig 4.13).

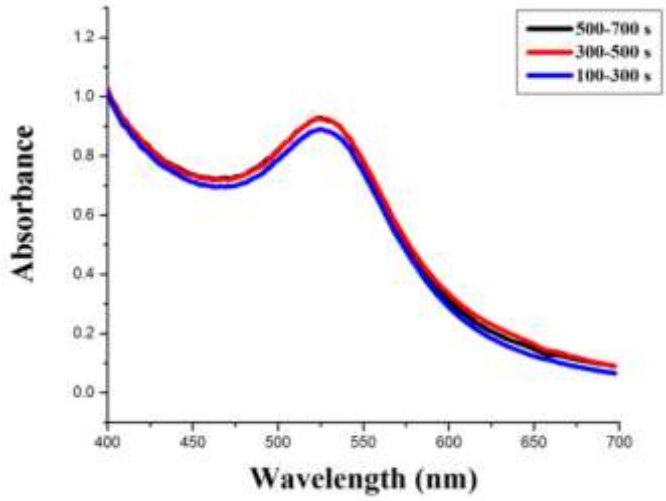

Figure 4.12: Visible spectra of gold nanoparticles synthesized in CFMR made of PDMS. Gold nanoparticle samples collected at different times to check the dynamics of reactor. The overlapping of UV-Vis spectra of samples collected at various time intervals (300-500 s, 500-700 s) verifies the steady state nature of the process.

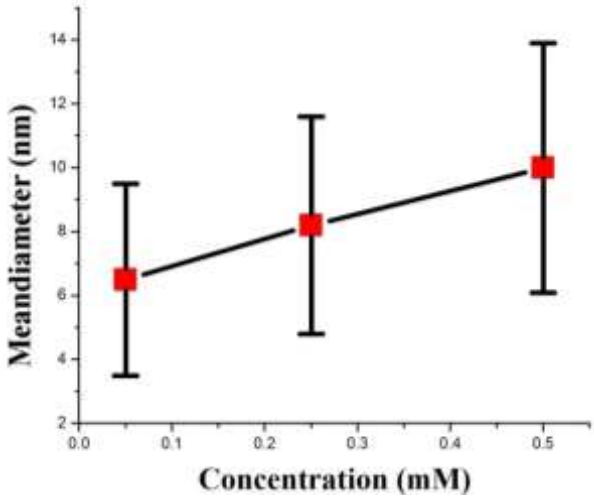

Figure 4.13: Schematic showing the variation of mean diameter of gold nanoparticles with overall concentration of gold synthesized in CFMR.

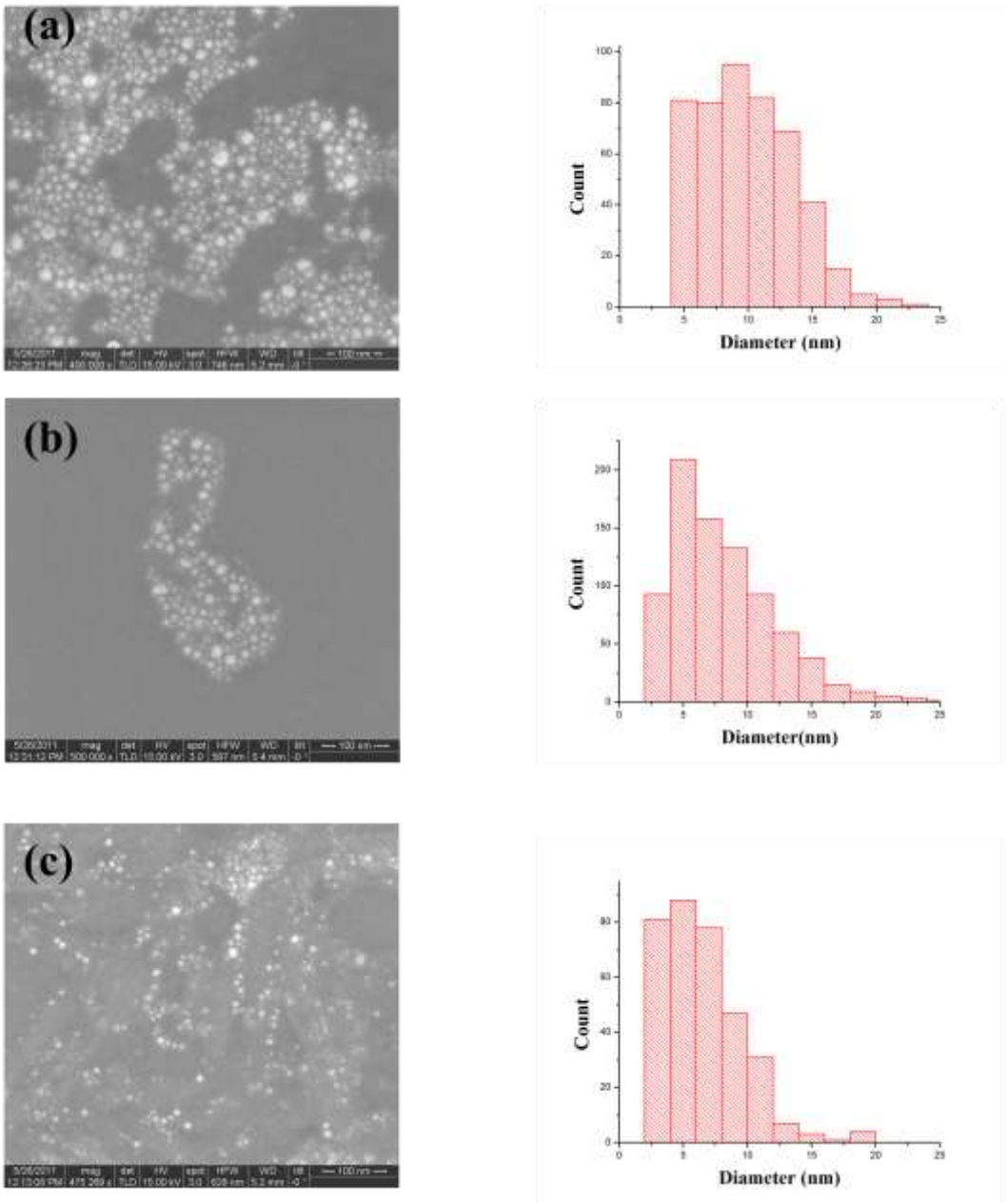

Figure 4.14: Representative SEM images and histograms of gold nanoparticles synthesized in CFMR by varying overall concentrations of gold salt (a) 0.5 mM, Particle size distribution 10±3.9nm (b) 0.25 mM, Particle size distribution 8.2 ±3.4 nm (d) 0.05 mM, Particle size distribution 6.5± 3.0nm.

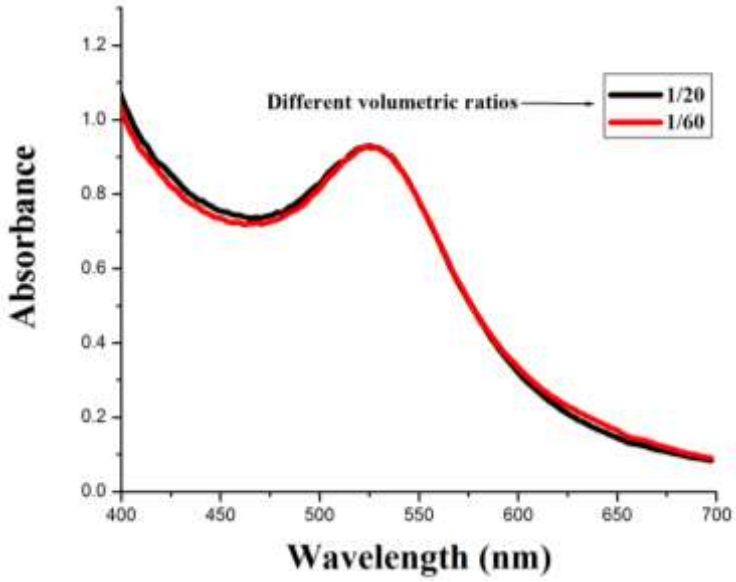

Figure 4.15: UV-Visible spectrum studies of gold nanoparticle synthesized in CFMR at different volumetric flow ratios to vary the diffusion times. Coincidence of UV-Visible spectrum of both diffusion times confirms that mean size and particle distribution remains same.

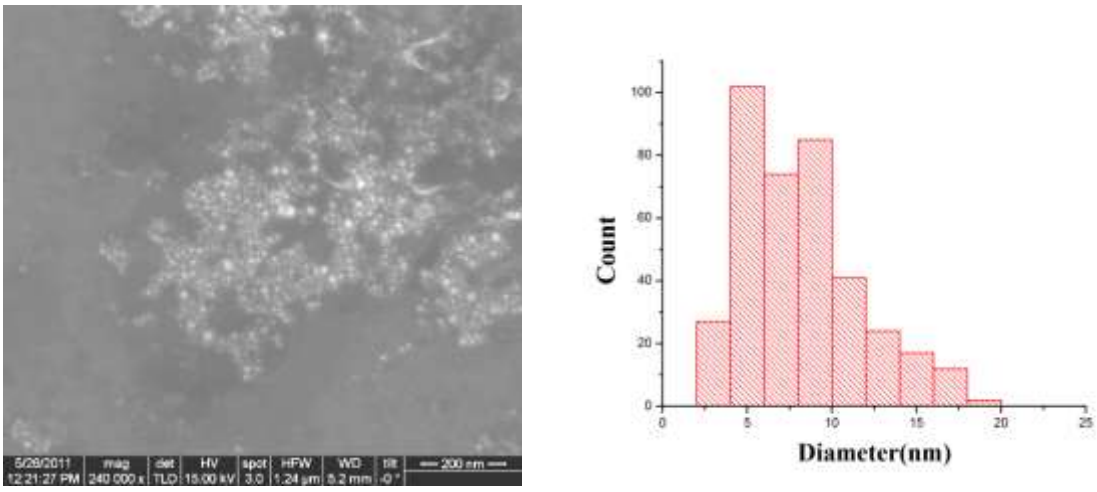

Figure 4.16: Representive SEM image and histogram of gold nanoparticle synthesized in CFMR by maintaining tannic acid flow rate at 45ml/hr where as chloroauric acid flow rate at 0.75 ml/hr ([HAuCl4=0.25 mM,[Tannic acid]=0.09 mM).Particle diametr found to be 8.2±3.5 nm.

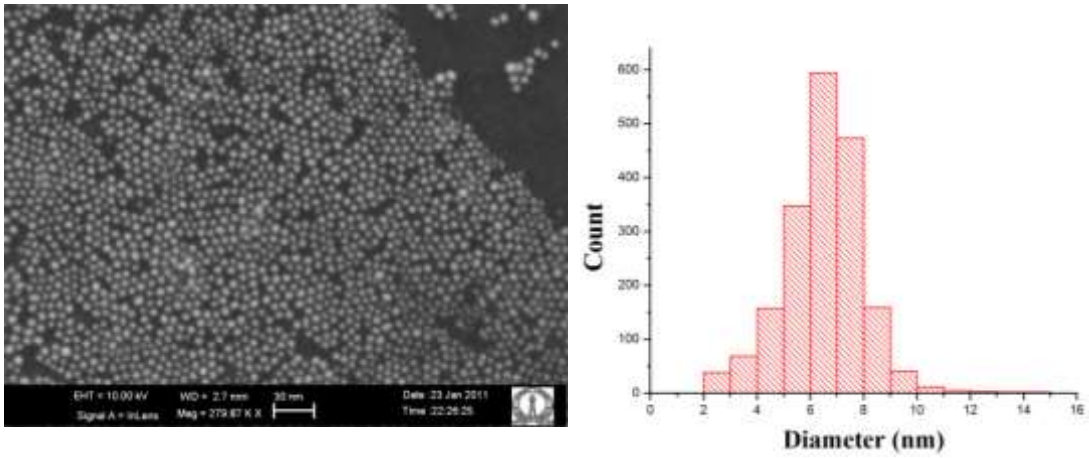

Figure 4.17: Representive SEM image and histogram of gold nanoparticle synthesized in batch by maintaining tannic acid concentration at 0.09 mM where as concentration of chloroauric is acid 0.25 mM.Particle diametr found to be 6.5±1.5 nm.

Table 4.2: Size distribution of gold nanoparticles synthesized at different diffusion times

Diffusion time	**Particle size distribution (nm)**	**Polydispersity (%)**
3.0 s (Batch)	6.5 ± 1.5	23
3.6 s (CFMR)	8.2 ± 3.4	41
9.0 s (CFMR)	8.2 ± 3.5	43

Similar to the results obtained for silver nanoparticle synthesis, the effect of varying the flow rate ratio is insignificant on particle size distribution of the synthesized collides (Fig 4.15, 4.16) (summarized in Table 4.2). Finally, Fig 4.17 shown the FE-SEM image of gold nanoparticles synthesized using a batch reactor. The size of the particles is measure to be 6.5 ± 1.5 nm. At the lower mean size and polydispersity of the colloids synthesized in batch process shows that the differing pH environment in inner core of outer fluid plays a key role in determining particle size distribution of gold colloids synthesized by reduction of chloroauric acid. Also, the time taken for chloroauric acid species equilibration upon change in pH of environment is large and thus leads to coalescence irrespective of the core diameter. This suggests that the optimal value of the initial pH of chloroauric acid solution needed to minimize coalescence is different for batch[20] and continuous process.

Chapter 5 Conclusions and Future work

A robust and stable design for low cost fabrication of a tubular microreactor has been developed. It was observed that the co axial flow pattern is very sensitive to disturbances and the alignment of the two tubes is critical. The proposed fabrication method based on the use of PDMS and silica capillary helps to eliminate the effect of external disturbances. Gold and silver nanoparticles were synthesized in a continuous manner with the process achieving steady state within minutes. The particle size distribution of gold and silver were mainly determined by the precursor concentrations and pH (chemistry), whereas the flow parameters such as total flow rate and outer to inner flow rate ratio had negligible effect. This lack of sensitivity to flow parameters enables robust operation of the reactor without the need for sophisticated control equipment to maintain product quality i.e. particle size distribution. The presence of different pH environment in the case of gold nanoparticles synthesis leads to larger polydispersity (as compared to bulk). This aspect needs future investigation and could possibly be overcome by optimizing the initial pH of chloroauric acid solution.

References

1. Sleightholm L, Zambre A, Chanda N, Afrasiabi Z, Katti K, Kannan R. New nanomedicine approaches using gold-thioguanine nanoconjugates as metallo-ligands. *Inorganica Chimica Acta.* 2011;372(1):333-339.

2. Dong X, Huang W, Chen P. In Situ Synthesis of Reduced Graphene Oxide and Gold Nanocomposites for Nanoelectronics and Biosensing. *Nanoscale Research Letters.* 2011;6(1):1-6.

3. Tamáska I, Dobrik G, Nemes-Incze P, et al. Bioinspired photonic nanoarchitectures from graphitic thin films. *Thin Solid Films.* 2011;519(12):4078-4081.

4. Farokhzad OC, Langer R. Impact of nanotechnology on drug delivery. *ACS Nano.* 2009;3(1):16-20.

5. Lee JG, Chen CL, Choi CJ, Mori H. In situ HREM study on sublimation-induced phase change in nanometer-sized gold and silver particles2010.

6. van Zalinge H, van Delft FCMJM, Weemaes RGR, van Thiel EFMJ, Snijder J, Nicolau DV. Nanoscale electrode gaps to study single molecule conduction. *Microelectronic Engineering.* 2011.

7. Méndez-Cruz M, Ramírez-Solís J, Zanella R. CO oxidation on gold nanoparticles supported over titanium oxide nanotubes. *Catalysis Today.* 2011;166(1):172-179.

8. Kooij ES, Ahmed W, Zandvliet HJW, Poelsema B. Localized plasmons in noble metal nanospheroids. *Journal of Physical Chemistry C.* 2011;115(21):10321-10332.

9. Zhao S, Ramakrishnan G, Su D, Rieger R, Koller A, Orlov A. Novel photocatalytic applications of sub-nanometer gold particles for environmental liquid and gas phase reactions. *Applied Catalysis B: Environmental.* 2011;104(3-4):239-244.

10. Tuchina ES, Ratto F, Khlebtsov BN, et al. Combined near infrared photothermolysis and photodynamic therapy by association of gold nanoparticles and an organic dye2011.

11. Abalde-Cela S, Aldeanueva-Potel P, Mateo-Mateo C, Rodríguez-Lorenzo L, Alvarez-Puebla RA, Liz-Marzán LM. Surface-enhanced Raman scattering biomedical applications of plasmonic colloidal particles. *Journal of the Royal Society Interface.* 2010;7(SUPPL. 4):S435-S450.

12. Geoffrey C. Bond CL, David T. Thompson. Catalysis by gold. Vol 6. London2006.

13. Lee JS, Kim YM, Kwon JH, et al. Multilevel data storage memory devices based on the controlled capacitive coupling of trapped electrons. *Advanced Materials.* 2011;23(18):2064-2068.

14. Cooper JS, Raguse B, Chow E, Hubble L, Müller KH, Wieczorek L. Gold nanoparticle chemiresistor sensor array that differentiates between hydrocarbon fuels dissolved in artificial seawater. *Analytical Chemistry.* 2010;82(9):3788-3795.

15. Zhao CX, He L, Qiao SZ, Middelberg APJ. Nanoparticle synthesis in microreactors. *Chemical Engineering Science.* 2011;66(7):1463-1479.

16. Cao G. NANOSTRUCTURES &NANOMATERIALS. London: Imperial College Press; 2004. Accessed 26 March 2004.

17. Rudin T, Wegner K, Pratsinis SE. Uniform nanoparticles by flame-assisted spray pyrolysis (FASP) of low cost precursors. *Journal of Nanoparticle Research.* 2011:1-11.

18. Turkevich J, Stevenson PC, Hillier J. A study of the nucleation and growth processes in the synthesis of colloidal gold. *Discussions of the Faraday Society.* 1951;11:55-75.

19. Brust M, Walker M, Bethell D, Schiffrin DJ, Whyman R. Synthesis of thiol-derivatised gold nanoparticles in a two-phase liquid-liquid system. *Journal of the Chemical Society, Chemical Communications.* 1994(7):801-802.

20. Sivaraman SK, Kumar S, Santhanam V. Room-temperature synthesis of gold nanoparticles - Size-control by slow addition. *Gold Bulletin.* 2010;43(4):275-286.

21. DeMello J, DeMello A. Microscale reactors: Nanoscale products. *Lab on a Chip - Miniaturisation for Chemistry and Biology.* 2004;4(2):11N-15N.

22. Lin XZ, Terepka AD, Yang H. Synthesis of silver nanoparticles in a continuous flow tubular microreactor. *Nano Letters.* 2004;4(11):2227-2232.

23. Jähnisch K, Hessel V, Löwe H, Baerns M. Chemistry in Microstructured Reactors. *Angewandte Chemie - International Edition.* 2004;43(4):406-446.

24. Wagner J, Köhler JM. Continuous synthesis of gold nanoparticles in a microreactor. *Nano Letters.* 2005;5(4):685-691.

25. Hassan. A. A. SO, Cabuil. V and Tabeling. P. Synthesis of iron oxide nanoparticles in a microfluidic device: preliminary results in a co-axial flow millichannel. *Chemical Communications.* 2008:1783-1785.

26. Parveen.B. *Room temperature synthesis gold nanoparticles*, Indian Institute of Science; 2010.

27. Shalom D, Wootton RCR, Winkle RF, et al. Synthesis of thiol functionalized gold nanoparticles using a continuous flow microfluidic reactor. *Materials Letters.* 2007;61(4-5):1146-1150.

28. Verma MKS, Majumder A, Ghatak A. Embedded template-assisted fabrication of complex microchannels in PDMS and design of a microfluidic adhesive. *Langmuir.* 2006;22(24):10291-10295.

29. Wagner J, Kirner T, Mayer G, Albert J, Köhler JM. Generation of metal nanoparticles in a microchannel reactor. *Chemical Engineering Journal.* 2004;101(1-3):251-260.

30. He ST, Liu YL, Maeda H. Controlled synthesis of colloidal silver nanoparticles in capillary micro-flow reactor. *Journal of Nanoparticle Research.* 2008;10(SUPPL. 1):209-215.

31. DeMello AJ. Control and detection of chemical reactions in microfluidic systems. *Nature.* 2006;442(7101):394-402.

32. Luty-Błocho M, Fitzner K, Hessel V, et al. Synthesis of gold nanoparticles in an interdigital micromixer using ascorbic acid and sodium borohydride as reducers. *Chemical Engineering Journal.* 2011;171(1):279-290.

33. Gómez-De Pedro S, Puyol M, Alonso-Chamarro J. Continuous flow synthesis of nanoparticles using ceramic microfluidic devices. *Nanotechnology.* 2010;21(41).

34. Takagi M, Maki T, Miyahara M, Mae K. Production of titania nanoparticles by using a new microreactor assembled with same axle dual pipe. *Chemical Engineering Journal.* 2004;101(1-3):269-276.

35. Pan Y, Yao J, Zhang L, Xu N. Preparation of Ultrafine Zeolite A Crystals with Narrow Particle Size Distribution Using a Two-Phase Liquid Segmented Microfluidic Reactor. *Industrial and Engineering Chemistry Research.* 2009;48(18):8471-8477.

36. Sivaraman SK, Elango I, Kumar S, Santhanam V. A green protocol for room temperature synthesis of silver nanoparticles in seconds. *Current Science.* 2009;97(7):1055-1059.

37. Jain V. *Synthesis of gold nanoparticles in spinning bowl-spinning disk reactor*: Indian Institute of science;2010.

38. Öncül AA, Sundmacher K, Seidel-Morgenstern A, Thévenin D. Numerical and analytical investigation of barium sulphate crystallization. *Chemical Engineering Science.* 2006;61(2):652-664.

39. Tsuji M, Miyamae N, Hashimoto M, et al. Shape and size controlled synthesis of gold nanocrystals using oxidative etching by AuCl4 - and Cl- anions in microwave-polyol process. *Colloids and Surfaces A: Physicochemical and Engineering Aspects.* 2007;302(1-3):587-598.

40. Villanueva-Luna AE, Santiago-Alvarado A, Castro-Ramos J, et al. Fabrication and characterization of phantoms made of polydimethylsiloxane (PDMS)2011.

41. Yuen PK, Su H, Goral VN, Fink KA. Three-dimensional interconnected microporous poly(dimethylsiloxane) microfluidic devices. *Lab on a Chip - Miniaturisation for Chemistry and Biology.* 2011;11(8):1541-1544.

42. Rao H, Zhang Z, Song C, Qiao T. Polydimethylsiloxane/liquid crystal cross-linked membranes: Preparation, characterization and oxygen transport properties. *Reactive and Functional Polymers.* 2011;71(5):537-543.

Appendix-A

A.1 Synthesis of gold nanoparticles in coaxial microreactors (with PDMS reservoirs)

We employed reservoirs between syringe pump and fluid lines to maintain coaxial flow (Fig A.1, A.2). The reason behind arranging the reservoir is to dampen the oscillations of syringe pump. Syringe pump oscillations are attributed due to stop-start motion of stepper motor. Gold nanoparticles were synthesized in CFMR by maintaining tannic acid flow rate at 36 mL/h where as gold at 3 mL/h. Concentration of chloroauric acid and tannic acid were maintained at 0.13 mM, 0.5 mM respectively. Studies of spectra (Fig A.3) showed that particles were growing with time. However, reactor did not reach steady state even after 10 min. Transmission electron microscopy (TEM) was used for further characterization of nanoparticles.

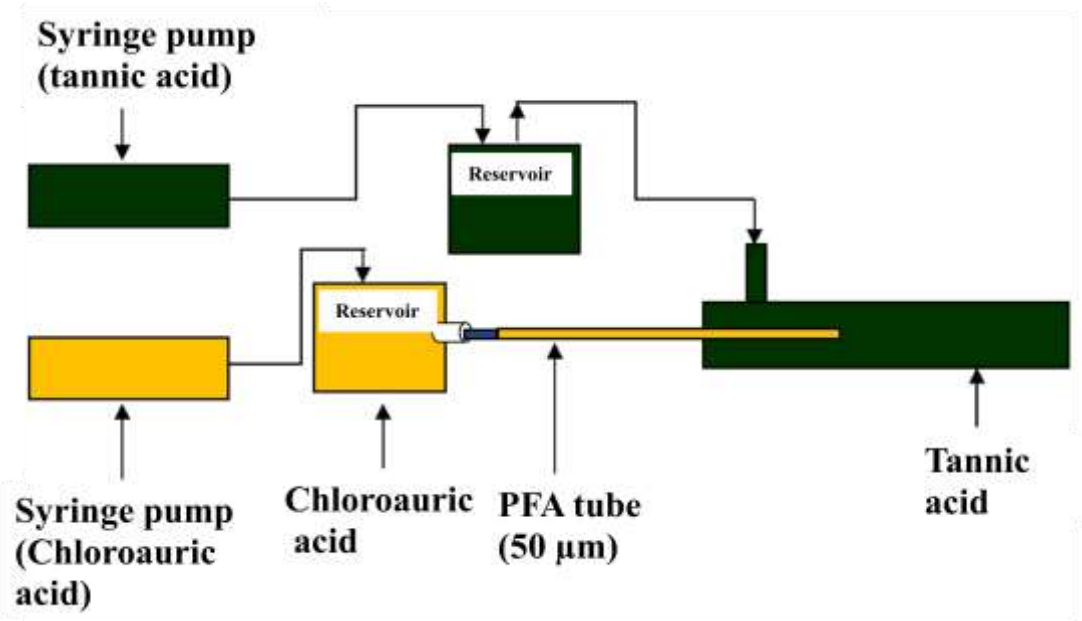

Figure A.0.1: Schematic showing the experimental setup of co axial flow microreactor. Two PDMS reservoirs deployed between syringe pump and fluid lines to dampen the oscillations.

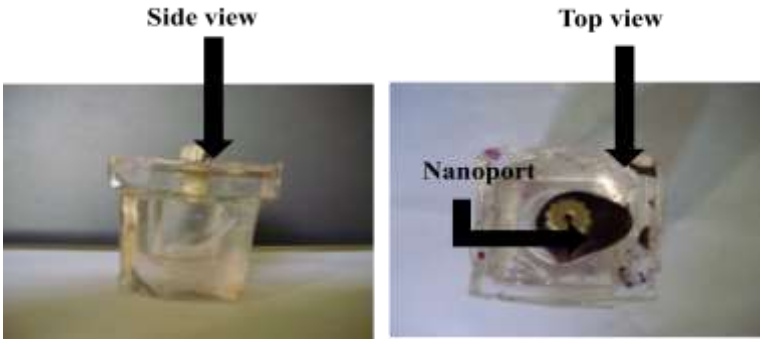

Figure 0.2: Digital micro graph of Gold salt -PDMS reservoir. Nanoport was embedded in PDMS used to connect 50 µm PFA tube.

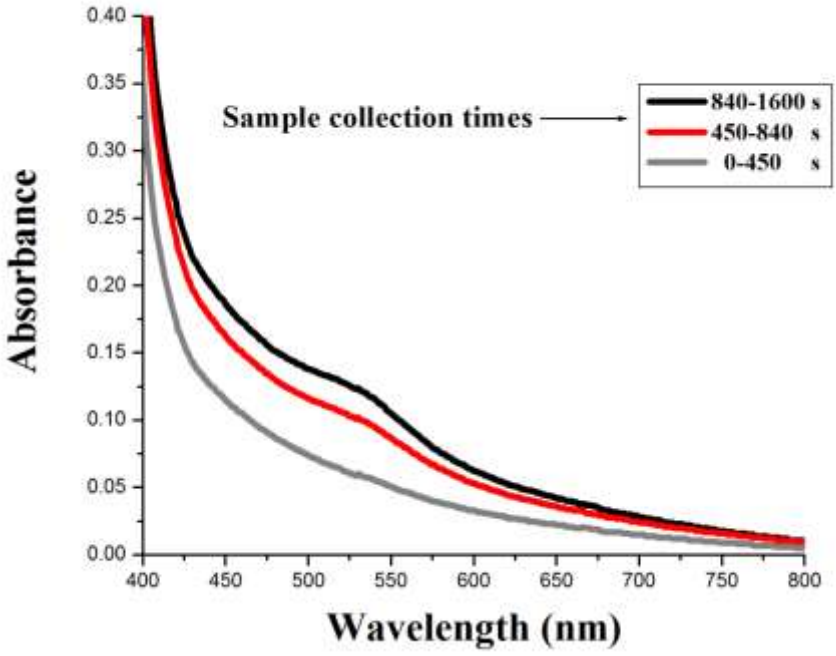

Figure 0.3: UV Visible spectra of gold nanoparticles synthesized in CFMR. Samples were collected at different times to check the dynamics of the reactor. Interestingly, Reactor does not reached steady state even after 10 min also.

Clemex software was used to calculate particle size distribution from TEM images. Particle size found to be 3.1 ± 0.8 nm for gold nanoparticles collected at 450-840 s (Fig A.4).

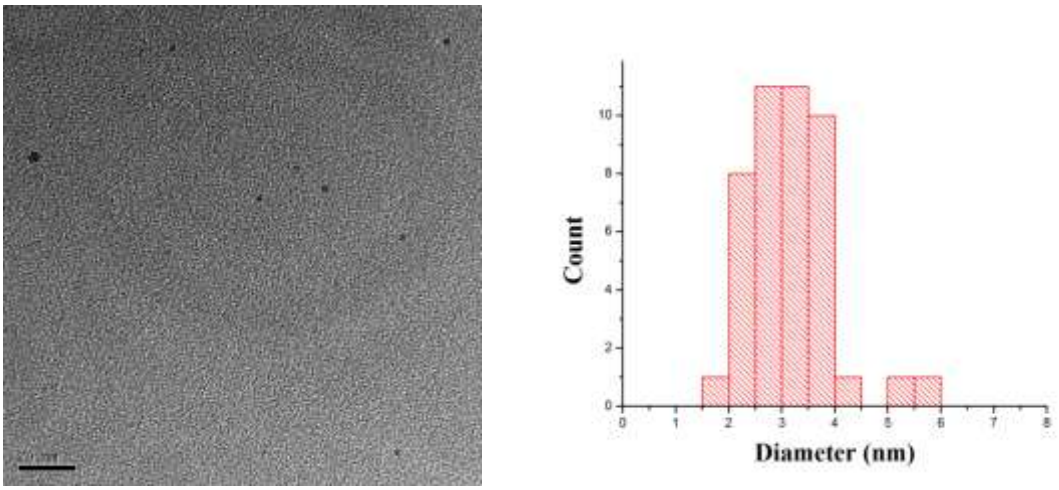

Figure 0.4: Representive TEM image and histogram of gold nanoparticles synthesized in CFMR by operating flow rates at 36 ml/hr for tannic acid where as3ml/hr for chloroauric acid. Particle size distribution found to be 3.1±0.8 nm.

Unsteady state of continuous flow process was attributed due to performance of PDMS reservoirs. Liquid has to pass through huge resistance to flow through 50µm channel from 4mm nanoport in the case of gold salt reservoir. This resistance makes PDMS reservoirs to swell and this leads to accumulation of some amount results and in non uniformity in the fluid flow through 50 µm micro channel; which in turn results in to unsteady state of the reactor. On the other hand, there was no problem with tannic acid reservoir because it was connected directly to reservoir through 1 mm tube. Reason to observe the smaller nanoparticle is that less amount of gold salt pumped along with tannic acid during experiment. Deploying reservoirs between fluid lines is not a good idea to dampen syringe pump oscillations. It is better to connect

flow lines directly to the smaller syringes. They have the capability of reducing oscillations of syringe pump.

A.2 Fabrication of PDMS based inlet manifold

Molding a polymer around a desired shape is simple and rapid method to obtain polymer based prototypes. Co axial flow microreactor (CFMR) fabricated using glass as material (Fig A.4) and CFMR used as mould to fabricate PDMS based inlet manifold. Bubble free PDMS, which is the mixture of SYLGARD 184 silicone elastomer base and curing agent (10:1 by weight), was poured in the aluminum mould (Fig A.5). It was then kept in an oven for curing at $60^{o}C$ for four hours. After curing, Hexane and heptanes were used to swell the PDMS cross linked network to remove the CFMR from it. PDMS block was allowed to deswell in ethanol and followed by five hours of continuous heating in oven at $60^{0}C$ to evaporate ethanol and heptane solvents from it.

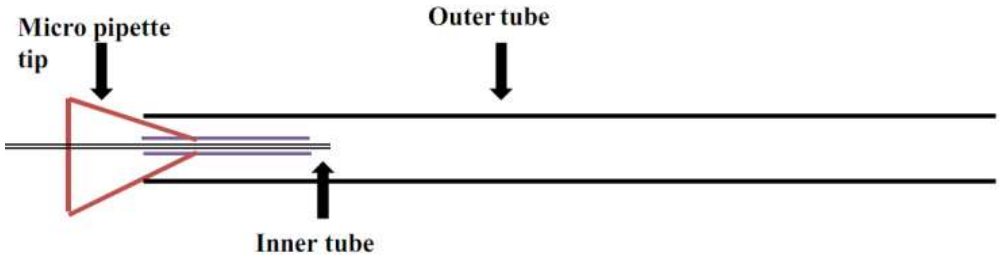

Figure 0.5: Schematic of Co axial flow micro reactor, which is used as a mold for fabricating PDMS based inlet manifold.

Glass tube as an outer tube with 30 cm length and 2 mm OD was inserted carefully in it. PFA tube with glass capillary was inserted in concentric micropipette tip and PDMS was poured in it to give enough strength to glass capillary. Blunt needle with sharp edge was used to make holes to the PDMS based inlet manifold. These holes allow the outer fluid to flow through outer tube of CFMR (Fig A.7).

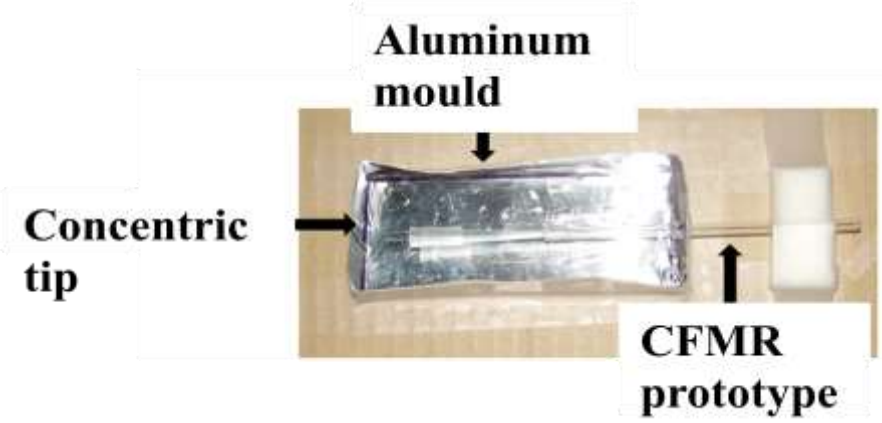

Figure 0.6 : Snapshot of PDMS mould with CFMR. Aluminum sheet was used for preparing PDMS mould.

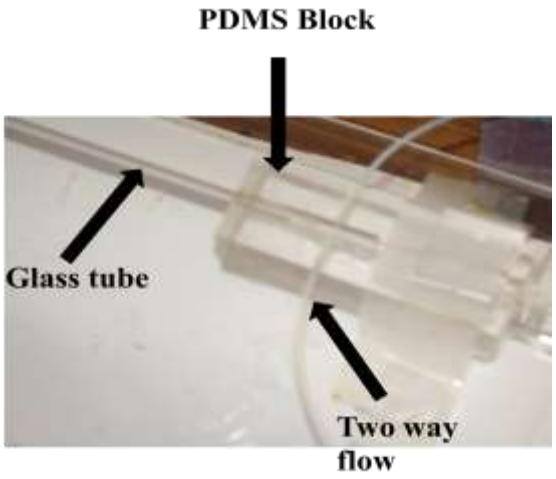

Figure 0.7: Snapshot of CFMR with PDMS Block. Two inlets are arranged for outer fluid flow through outer tube.

A.3 Theoretical calculation of inner core diameter

Diameter of inner core is calculated by neglecting the diffusion. Inner diameter calculated as follows

Overall flow rate through CFMR $Q = Q_{in} + Q_{Out}$

Here Q_{in}= Inner fluid flow rate through inner tube

Q_{out}=Outer fluid flow rate through outer tube

In laminar 1-D flow

$$Q = \left(\frac{V_{max}}{2}\right)\pi R^2 \quad \text{(A.1)}$$

Inner fluid flow rate can be represented as

$$Q_{in} = \int_0^{r_i} 2\pi v(r)dr \quad \text{(A.2)}$$

Here V(r) =Velocity of fluid in along the flow direction

$$V(r) = V_{max}\left(1 - \frac{r^2}{R^2}\right) \quad \text{(A.3)}$$

Substitute equation A.2 in equation A.1

$$Q_{in} = 2\pi V_{max}\int_0^{r_i}\left(r - \frac{r^3}{R^2}\right)dr$$

$$= 2\pi V_{max}\left(\frac{r_i^2}{2} - \frac{r_i^4}{4R^2}\right) \quad \text{(A.4)}$$

Here V_{max}=Velocity at the center of the pipe, r_i=expected inner radius of inner tube, R=Inner radius of outer tube.

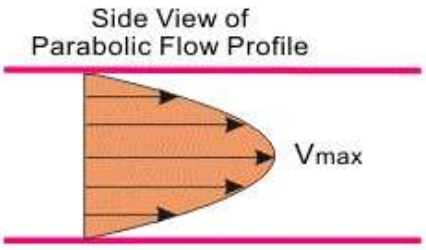

Figure 0.8 : Velocity distribution in CFMR along the cross section after transition length (2mm away from point confluence).

Substitute equation A.1 in equation A.4,

$$Q_{in} = 2\pi\left(\frac{2Q}{\pi R^2}\right)\left(\frac{r_i^2}{2} - \frac{r_i^4}{4R^2}\right) \quad \text{(A.5)}$$

Here $Q = Q_{in} + 60Q_{in}$

R= 1.2 mm substitute these values in equation – (5)

It gives r_i= 100 µm and D_t= 200 µm.